Received: 18 October 2021 | Revised: 4 December 2021 | Accepted: 6 December 2021

DOI: 10.1111/pce.14263

ORIGINAL ARTICLE

Plant, Cell & Environment | WILEY

# The rice heavy-metal transporter OsNRAMP1 regulates disease resistance by modulating ROS homoeostasis

Chuanliang Chu[1] | Renyan Huang[1] | Liping Liu[1] | Guilin Tang[1] | Jinghua Xiao[1] | Heejin Yoo[2] | Meng Yuan[1]

[1]National Key Laboratory of Crop Genetic Improvement, National Center of Plant Gene Research, Hubei Hongshan Laboratory, Huazhong Agricultural University, Wuhan, China

[2]Department of Plant Biology, Ecology, and Evolution, Oklahoma State University, Stillwater, Oklahoma, USA

**Correspondence**

Meng Yuan, National Key Laboratory of Crop Genetic Improvement, Hubei Hongshan Laboratory, Huazhong Agricultural University, Wuhan 430070, China.
Email: myuan@mail.hzau.edu.cn

**Funding information**

National Natural Science Foundation of China, Grant/Award Numbers: 31821005, 31871946, 32172421; National Science Foundation of Hubei Province, Grant/Award Number: 2020CFA058; Fundamental Research Funds for the Central Universities, Grant/Award Number: 2662019FW006

## Abstract

Crop diseases threaten food security and sustainable agriculture. Consumption of crops containing nonessential toxic metals leads to health risks for humans. Therefore, cultivation of disease-resistant and toxic metal-safe crops is a double-gain strategy that can contribute to food security. Here, we show that rice heavy-metal transporter OsNRAMP1 plays an important role in plant immunity by modulating metal ion and reactive oxygen species (ROS) homoeostasis. *OsNRAMP1* expression was induced after pathogenic bacteria and fungi infections. The *osnramp1* mutants had an increased content of $H_2O_2$ and activity of superoxide dismutase, but decreased activity of catalase, showing enhanced broad-spectrum resistance against bacterial and fungal pathogens. RNA-seq analysis identified a number of differentially expressed genes that were involved in metal ion and ROS homoeostasis. Altered expression of metal ion-dependent ROS-scavenging enzymes genes and lower accumulation of cations such as Mn together induced compromised metal ion-dependent enzyme-catalysing activity and modulated ROS homoeostasis, which together contributed towards disease resistance in *osnramp1* mutants. Furthermore, the *osnramp1* mutants contained lower levels of toxic heavy metals Cd and Pb and micronutrients Ni and Mn in leaves and grains. Taken together, a proof of concept was achieved that broad-spectrum disease-resistant and toxic heavy-metal-safe rice was engineered by removal of the *OsNRAMP1* gene.

**KEYWORDS**

disease resistance, *Oryza sativa*, *OsNRAMP1*, toxic elements, transporter

## 1 | INTRODUCTION

Consumption of crops containing nonessential toxic elements leads to potential health risks for humans. An ideal crop for human health should be enriched with essential mineral elements, but with negligible toxic elements in the edible parts (Clemens & Ma, 2016; Huang et al., 2020). For example, cadmium (Cd) and lead (Pb) are nonessential toxic heavy elements that should be ideally not present in grains. Nickel (Ni) and manganese (Mn) are essential micronutrients that should be present in grains in precise quantities because they have severe side effects when overdigested or when there is lower intake by humans. Both nonessential toxic elements and essential micronutrients are absorbed by plant roots from the soil and then transported to vegetative organs or grains by a large number of transporters. The strategy of blocking the process of transportation of toxic elements from roots to shoots or from vegetative organs to

Chuanliang Chu and Renyan Huang contributed equally to this study.

  

grains has been achieved by the manipulation of mineral transporters in several crops. This strategy is agriculturally critical to cultivate toxic heavy-metal-safe varieties (Huang et al., 2020).

Heavy-metal ion transporters in plants have been reported to play a role in disease resistance, which depends on the types or storage tissues of metal ions (Fones & Preston, 2013). The over-accumulation or deficiency of metal ions can alter the activity of metal cation-dependent enzymes, resulting in the modified homoeostasis of metabolic pathways in plants (Clemens & Ma, 2016). Metal ions are not only essential for modulating reactive oxygen species (ROS) homoeostasis but also important for plant defences and restricting pathogen proliferation. For example, rice OsCNGC9 encoding a channel with calcium ($Ca^{2+}$) influx capacity regulates resistance to fungal pathogen *Magnaporthe oryzae* by pumping $Ca^{2+}$ into cells to trigger ROS burst (J. Wang et al., 2019). Rice potassium ($K^+$) channel OsAKT1 positively regulates rice resistance against *M. oryzae* by transporting $K^+$ into cells to initiate ROS burst (X. Shi et al., 2018). Rice copper transporters OsCOPT1 and OsCOPT5 can redistribute $Cu^{2+}$ to xylem vessels to restrict *Xanthomonas oryzae* pv. *oryzae* (*Xoo*) proliferation (Yuan et al., 2010). Therefore, the host plants adopt different strategies by controlling the expression of metal ion transporters to fine-tune metabolic homoeostasis to limit the proliferation of pathogens.

The natural resistance-associated macrophage proteins (NRAMPs) play important roles in the uptake, transportation and detoxification of multiple metal ions in a wide range of living beings from bacteria to humans (Bozzi & Gaudet, 2021). Rice genome encodes seven NRAMP proteins (Mani & Sankaranarayanan, 2018), and some of them have been found to have transporting activity on different metal ions. The plasma membrane-localized transporter OsNRAMP1 can transport iron (Fe), Cd, Mn and arsenic (As) in heterologous yeast (Chang et al., 2020; Takahashi et al., 2011; Tiwari et al., 2014), and contributes to the uptake of Mn and Cd in rice (Chang et al., 2020; Takahashi et al., 2011). Consequently, the knockout of *OsNRAMP1* resulted in compromised uptake of Mn and Cd in root and attenuated accumulation of Mn and Cd in rice shoots and grains and increased sensitivity to Mn deficiency (Chang et al., 2020). In contrast, overexpression of *OsNRAMP1* increased Cd accumulation in rice leaves (Takahashi et al., 2011). OsNRAMP2 is a tonoplast-localized transporter that plays a role in Fe homoeostasis by transporting Fe from the rice vacuole to the cytosol (Y. Li et al., 2021). The plasma membrane-localized transporter OsNRAMP3 is responsible for Mn uptake and distribution to old tissues (Yamaji et al., 2013). OsNRAMP4 is a root plasma membrane aluminium (Al) transporter (J. Y. Li et al., 2014). The plasma membrane-localized transporter OsNRAMP5 is a major influx transporter for Mn, Fe and Cd (Sasaki et al., 2012). Overexpression of *OsNRAMP5* significantly decreased Cd accumulation in rice shoots and grains (Chang et al., 2020). OsNRAMP6, a plasma membrane-localized transporter, is involved in the uptake of Fe and Mn (Peris-Peris et al., 2017). OsNRAMP7 is colocalized with a quantitative trait locus transporting Fe and zinc (Zn) (Descalsota et al., 2018). Moreover, several rice *NRAMP* genes have different expression patterns in response to different hormonal treatments. The expression of *OsNRAMP1* was suppressed by jasmonic acid and abscisic acid, whereas *the* expression of *OsNRAMP2* was induced by jasmonic acid, abscisic acid and ethephon. *The expression of OsNRAMP3* was induced by abscisic acid (Zhou & Yang, 2004). In addition, some rice *OsNRAMP* genes have diverse expression patterns against pathogen infection. The expression of *OsNRAMP1* was suppressed by bacterial pathogen *Burkholderia glumae*, but induced by fungal pathogen *M. oryzae*. The expression of *OsNRAMP2* and *OsNRAMP3* was induced by *B. glumae* and *M. oryzae* (Zhou & Yang, 2004). *OsNRAMP6* expression was induced by *M. oryzae*. Therefore, the loss of function of *OsNRAMP6* conferred enhanced resistance against *M. oryzae* (Peris-Peris et al., 2017). However, whether *OsNRAMP1* plays a direct role in disease resistance, and the underlying molecular mechanisms are largely unknown.

Here, we report loss of function of *OsNRAMP1*-conferred resistance against both bacterial and fungal pathogens, which was possible due to altered ROS homoeostasis regulated by metal ion-dependent enzymes. Simultaneously, knockout of *OsNRAMP1* resulted in significantly attenuated accumulation of toxic heavy metals Cd and Pb and micronutrients Ni and Mn in rice grains. Our study could provide a new engineering strategy to improve the broad spectrum of disease resistance and toxic metal-safe rice by controlling the expression level of *OsNRAMP1*.

## 2 | MATERIALS AND METHODS

### 2.1 | Plant materials and growth conditions

Rice (*Oryza sativa* ssp. *Geng*) Zhonghua 11 (ZH11), Mudanjiang 8 (MDJ8) and transgenic line Rb49, which carries a disease resistance gene *Xa3/Xa26* in MDJ8 (Sun et al., 2004), were used for experiments. The *osnramp1* mutants and *OsNRAMP1*-overexpressing (*OsNRAMP1*-OE) plants were generated in ZH11 as described below. Germinated seedlings were planted in the paddy field of Huazhong Agricultural University in Wuhan under natural conditions at temperatures of 26–35°C at day and 21–32°C at night, with relative humidity at 70–95%Rh. Fertilizers were applied (per hectare) as follows: 90 kg of N, 45 kg of P and 72 kg of K (M. Yang et al., 2018). Rice plants from the vegetative stage to the reproductive stage were watered daily, and a minimum layer of 2 cm of water was maintained. Fifteen soil samples from the paddy field were collected randomly for the analysis of soil nutrients (metal ion components and concentrations, pH values). The metal ion components and concentrations of soil were as follows: As (12.47 mg/kg), Cd (0.14 mg/kg), Cu (26.40 mg/kg), Fe (38.11 g/kg), Mg (3.98 g/kg), Mn (0.63 g/kg), Mo (0.15 mg/kg), Pb (27.75 mg/kg) and Zn (67.68 mg/kg). The pH of the soil was 6.6. The irrigation water was sampled semimonthly for the analysis of water nutrients (metal ion components and concentrations, pH values). The metal ion components and concentrations of irrigation water were as follows: As (2.32 μg/L), Cu (0.84 μg/L), Mg (10.21 mg/L), Mn (3.40 μg/L), Mo (0.57 μg/L) and Pb (0.05 μg/L). The pH of irrigation water was 6.5.

## 2.2 | Generation of constructs and transgenic plants

The CRISPR/Cas9 strategy was used to knock out the *OsNRAMP1* gene in japonica rice variety ZH11. Target sites were designed using the web tool CRISPR-P (http://crispr.hzau.edu.cn/CRISPR2/). Two 20-bp sgRNA targeting the sixth and seventh exons of *OsNRAMP1*, respectively, were constructed on the sgRNA expression cassettes of OsU3 and OsU6a by overlapping polymerase chain reaction (PCR), and then the Gibson Assembly cloning method was used to assemble the multiple sgRNA expression cassettes into the pYLCRISPR/Cas9 expression vector (X. Ma et al., 2015). The full-length cDNA of *OsNRAMP1* was amplified from ZH11 using the specific primers (Table S1) and then inserted into the pU1301 vector using the restriction-ligation method (Yuan et al., 2010). The insertion fragments of all the vectors were examined by DNA sequencing using vector-specific primers (Table S1). These constructs were transformed into *Agrobacterium tumefaciens* strain EHA105 by electroporation, and further transformed into rice calli from mature embryos of ZH11 by *Agrobacterium*-mediated transformation (Yuan et al., 2010). Transgenic lines were selected by hygromycin resistance. The positive lines of *OsNRAMP1*-OE plants were verified by PCR using a vector-specific primer and a gene-specific primer. The *osnramp1* mutants were verified by sequencing the genome DNA of *OsNRAMP1*. The homozygous *osnramp1* T2 or T3 generations were used in the experiments.

## 2.3 | Pathogen inoculation

To evaluate the response of transgenic plants to *Xoo*, five to seven uppermost fully expanded flag leaves of each plant were inoculated with *Xoo* at the booting (panicle development) stage. Briefly, *Xoo* stocks were streaked on nutrient agar medium (1 g/L yeast extract, 3 g/L beef extract, 5 g/L polypeptone, 10 g/L sucrose and 20 g/L agar) and incubated at 28°C for 2 days. Cells were harvested from the agar medium, suspended in sterilized water and adjusted to an optical density of 0.5 at 600 nm. Rice leaves were inoculated with *Xoo* using the leaf-clipping method (Yuan et al., 2016). *Xoo* used in this study included six Philippine strains (PXO61, PXO71, PXO99, PXO112, PXO341 and PXO347) and two Chinese strains (Zhe173 and KS 1-21), which were isolated from different regions showing virulence on ZH11 (Hui et al., 2019). Disease was scored by measuring the lesion length at 14 days after inoculation. The bacterial growth rate in rice leaves was determined by counting colony-forming units (Yuan et al., 2016).

To elucidate the response of transgenic plants against *X. oryzae* pv. *oryzicola* (*Xoc*), 5–10 fully expanded leaves of each plant were inoculated with *Xoc* at the tillering stage. *Xoc* stocks were streaked on nutrient agar medium and incubated at 28°C for 2 days. Cells were harvested from the agar medium, suspended in sterilized water and adjusted to an optical density of 0.5 at 600 nm. Rice leaves were inoculated with *Xoc* using the penetration method (Hui et al., 2019). Three *Xoc* strains used in this study were RH3, GX01 and HNB8-47 (Hui et al., 2019). Disease was scored by measuring the lesion length at 14 days after inoculation. The bacterial growth in rice leaves was determined by counting colony-forming units (Yuan et al., 2016).

To assess the response of transgenic plants to *M. oryzae*, rice leaves were inoculated with *M. oryzae* at the tillering stage. *M. oryzae* isolates were cultured on oatmeal tomato agar medium (40 g/L oatmeal, 15% tomato juice and 20 g/L agar) at 28°C for 4 days. Conidia were harvested from the medium, suspended in sterilized water containing 0.05% Tween-20 and adjusted to an optical density of $5.0 \times 10^5$ spores per millilitre. Rice leaves were inoculated with *M. oryzae* using the punch inoculation method (Xu et al., 2017). *M. oryzae* isolates used in this study were M2 and 08T17 (Xu et al., 2017). Disease was scored by measuring the lesion length at 7 days after inoculation. The fungal biomass in infected rice leaf was quantified using the threshold cycle value of *M. oryzae Pot2* DNA against the cycle value of rice genomic *ubiquitin* DNA (Park et al., 2012).

To evaluate the response of transgenic plants to *Ustilaginoidea virens*, rice panicles were inoculated with *U. virens* at the booting stage. *U. virens* isolates were cultured on potato sucrose medium (200 g/L potato and 16 g/L sucrose) at 28°C for 7 days. The mixture of mycelia and conidia formed was adjusted to an optical density of $10^6$ conidia per millilitre. Rice panicles were inoculated with *U. virens* using the needleless syringe-based injection method (Song et al., 2016). *U. virens* isolates used in this study were WH13 and TF14 (Song et al., 2016). Disease was scored by measuring the number of rice false smut balls per panicle at 14 days after inoculation. The fungal biomass in an infected rice floret was quantified using the threshold cycle value of *U. virens β-actin* DNA against the cycle value of rice genomic *GAPDH* DNA (Song et al., 2016).

## 2.4 | Gene expression analysis

For gene expression analysis, quantitative real-time PCR (RT-qPCR) was performed using the LightCycler® 480 SYBR Green I Master in the ABI 7500 Real-Time PCR System (Applied Biosystems). Total RNA was extracted using Trizol reagent (Invitrogen). An aliquot (5 μg) of total RNA was treated with RNase-free DNase I (Invitrogen) to remove potentially contaminating DNA, and then first-strand cDNA was reverse-transcribed from total RNA with the oligo$(dT)_{18}$ primer using M-MLV reverse transcriptase (Promega) according to the manufacturer's instructions. RT-qPCR was conducted using gene-specific primers (Table S2) that were designed using the primer analysis software Primer Express v3.0 (Applied Biosystems). The rice *actin* and *GAPDH* genes that were stably expressed in rice tissues upon pathogens challenges were used to standardize the relative RNA measures as inner controls (L. Wang et al., 2010). Each RT-qPCR assay was biologically repeated at least twice with similar results, with each repetition having three technical replicates (Yuan et al., 2016). Student's *t* test was used for the RT-qPCR analysis.

## 2.5 | RNA-seq analysis

Rice leaves at the booting stage of the *osnramp1-1* mutant and wild type were collected with three biological replicates. RNA extraction, quantification, library construction and Illumina HiSeq. 2500 platform-based sequencing were conducted by Novogene. Read quality of the raw data was evaluated by the FastQC application v0.11.2. Each paired-end library had insert size between 200 and 300 bp. After removing adapter sequences and low-quality reads by Cutadapt tool, clean sequence reads were mapped to the available rice Nipponbare genome (Release 7 of the MSU Rice Genome Annotation Project) using TopHat v2.0.12. Then, Cufflinks was applied to measure the transcript abundance and presented the expression of each transcript in FPKM (fragments per kilobase pair of exon model per million fragments mapped). The DESeq R package was used for differential expression analysis, that differentially expressed genes characterized by relative expression $\log_2FC \geq 1$ or $\log_2FC \leq -1$ and the false discovery rate (FDR) < 0.05 considered as differentially expressed genes (DEGs) (Hong et al., 2015). Software tools Goatools and KOBAS were used for the Gene Ontology (GO) and the Kyoto Encyclopedia of Genes and Genomes (KEGG) analysis with an adjusted *p* value cutoff of 0.05.

## 2.6 | Elemental analysis

Rice plants were grown in the paddy field; the leaves at the booting stage and grains at the mature stage were sampled and dried at 80°C for 5 days and ground to fine powders. About 0.2 g of dried powder of the leaf sample was digested with $HNO_3/HClO_4$ (85:15, vol:vol) and 0.2 g of dried powder of the grain sample was digested with high-purity $HNO_3$ in a MARS6 microwave with a gradient of temperature from 120°C to 180°C for 45 min. After dilution in deionized water, the concentrations of As, Cd, Cu, Fe, Mg, Mn, Mo, Ni, Pb and Zn were determined by inductively coupled plasma mass spectrometry (ICP-MS, Agilent 7700E) as described previously (M. Yang et al., 2018). Elemental concentration measurement was biologically repeated three times, with each repetition having three technical replicates. ICP-MS Quality Control Sample 2 containing 25 reference components was used for quality control (AccuStandard). The measured concentrations of reference elements were in good agreement with the certified value.

## 2.7 | DAB staining

Rice plants were grown in the paddy field up to the booting stage; the leaves that showed spontaneous lesions were collected and used for 3,3′-diaminobenzidine (DAB) staining according to a previously described protocol (Park et al., 2012). Leaves were vacuum-infiltrated with DAB solution and incubated for 12 h in the dark, followed by chlorophyll removal using 95% ethanol in a water bath at 60°C overnight.

## 2.8 | Histochemical assay

Rice plants were grown in the paddy field up to the booting stage; the leaves with spontaneous lesions were collected and frozen immediately in liquid nitrogen. The contents of hydrogen peroxide ($H_2O_2$), and the activities of catalase (CAT), superoxide dismutase (SOD), Cu/Zn-SOD, Mn-SOD and Fe-SOD were measured using assay kits following the manufacturer's instructions (Elabscience). The glutaredoxin (GRX) activity was determined using assay kits according to the manufacturer's instructions (Cayman Chemical). The GSH and GSSG contents were assayed using the GSH/GSSG Assay Kit (Beyotime). The Amplite™ Fluorimetric NADP/NADPH Ratio Assay Kit (AAT Bioquest) was used to extract and measure the contents of $NADP^+$ and NADPH, and the $NADPH/NADP^+$ ratio according to the manufacturer's instructions (Liu et al., 2018). Fluorescence was measured using a microplate reader (Tecan Infinite M200). All the histochemical assays were biologically repeated three times, with each repetition having three technical replicates.

## 2.9 | Measurement of ROS

ROS production in rice leaves upon pathogen-associated molecular patterns (PAMP) treatment was monitored using the luminol chemiluminescence assay. Wounding can cause ROS generation, whereas the accumulated ROS can be bleached after samples are incubated in sterile distilled water for 12 h (Park et al., 2012). Therefore, to eliminate wounding-induced ROS accumulation, rice leaves from 4-week-old plants grown in the paddy field were sampled and cut into 4-mm-diameter discs, and then preincubated in sterile distilled water for 12 h in the dark. After pre-incubation, the leaf discs were placed on a paper towel to remove excess water; they were submerged in 1.5-ml microcentrifuge tubes containing 100 µl of luminol, 1 µl of horseradish peroxidase (Jackson ImmunoResearch) and 10 µM flg22 or 1 µM chitin with water as a control. After the treatment, luminescence was measured continuously at 1-min intervals for 30 min using a luminometer (Tecan Infinite M200).

## 2.10 | Measurement of chlorophyll

Leaves of rice plants at the tillering and booting stages were sampled for chlorophyll measurements. Fresh leaves were cut into pieces, and 0.02 g of the materials was submerged into 1.5 ml of extraction solution (95% ethanol:pure acetone:water = 4.5:4.5:1) and placed in the dark for 12 h. The absorbance of the extract was measured spectrophotometrically at 645 and 663 nm. The concentrations of Chl a, Chl b and total Chl were calculated using Arnon's equations (Arnon, 1949).

## 2.11 | Agronomic traits analysis

The rice plants examined under natural field conditions were grown in normal rice-growing seasons in the Experimental Station of

Huazhong Agricultural University. Rice seeds were sown on the seed bed in mid-May, and then rice seedlings were transplanted to the field in mid-June and left until the harvest stage in October. Each transgenic line was planted in three replicates at three different plots, with a total of 150 plants (10 plants per row). The planting density was 16.5 cm between plants in a row, and the rows were 26 cm apart. The tiller number, flag leaf length, flag leaf width and panicle length were scored at the ripening stage. The grain length, grain width, grain number per panicle, seed setting rate, 1000-grain weight and yield per plant were measured at the high-throughput rice phenotyping facility when plants were completely mature (W. Yang et al., 2014).

## 3 | RESULTS

### 3.1 | *OsNRAMP1* expression is induced upon pathogen challenge in rice

*OsNRAMP1* was induced after bacterial pathogen *Xoo* infection according to our previous microarray transcriptome data (Hong et al., 2015). Here, we analysed the expression level of *OsNRAMP1* upon pathogen challenge using the RT-qPCR assay. Consistent with microarray data, *OsNRAMP1* was highly induced in rice variety MDJ8 after bacterial pathogen *Xoo* infection (Figure 1a). We also examined *OsNRAMP1* expression in transgenic line Rb49 carrying a major disease resistance (*R*) gene *Xa3/Xa26* against *Xoo* in MDJ8 (Sun et al., 2004). The expression patterns of *OsNRAMP1* after *Xoo* infection were similar in MDJ8 and Rb49, which showed compatible and incompatible interactions between rice and *Xoo*, respectively (Figure 1a). This result suggests that transcriptional induction of *OsNRAMP1* is independent of *R* gene recognition upon pathogen infection.

Among the seven members of the rice NRAMP family, only *OsNRAMP1* and *OsNRAMP3* showed increased expression against *Xoo* infection, whereas expressions of *OsNRAMP2*, *OsNRAMP5*, *OsNRAMP6* and *OsNRAMP7* were not induced in response to *Xoo* infection (Figure 1b). Transcriptional induction of *OsNRAMP1* was much higher than that of *OsNRAMP3*, suggesting that *OsNRAMP1* plays an important role in immune response.

To evaluate whether *OsNRAMP1* expression is also induced by other bacterial pathogens or fungal pathogens, we analysed the *OsNRAMP1* expression pattern against different pathogen infections along with $H_2O$ inoculation as a mock control. Compared to mock inoculation, *Xoo* infection induced *OsNRAMP1* expression with a highest level at 8 h post infection (hpi) (Figure 1c). *OsNRAMP1* expression was also upregulated after bacterial pathogen *Xoc* infection, with a peak at 12 hpi (Figure 1d). Similarly, the expression of *OsNRAMP1* was significantly induced when rice was challenged with two fungal pathogens, *M. oryzae* and *U. virens*, with the highest levels at 48 and 72 hpi, respectively (Figure 1e,f). *OsNRAMP1* shows the highest expression levels at different time points in response to different pathogens, which is possibly attributable to different infection or response modes of these bacterial pathogens and fungal pathogens. Taken together, these results indicate that *OsNRAMP1* expression is induced upon different pathogen challenges.

### 3.2 | The *osnramp1* mutation triggers rice resistance to *Xoo*

To investigate the functional role of *OsNRAMP1* in disease resistance, we generated knockout lines of *OsNRAMP1* by CRISPR/Cas9-mediated mutagenesis in ZH11. Two sgRNAs targeting the sixth and seventh exons of *OsNRAMP1*, respectively, were designed for Cas9 cleavage and the construct was introduced into rice variety ZH11 by *Agrobacterium*-mediated transformation (Figure S1a). Eight heterozygous mutation T0 lines were obtained by sequencing the PCR-amplified target regions from a total of 13 transgenic plants. The homozygous mutants were obtained in T1 generation; among them, two mutants designated *osnramp1-1* and *osnramp1-2*, which contained large fragment deletions between the two targeting sites, were selected for further analysis (Figure S1b). The *osnramp1-1* and *osnramp1-2* mutants had 272-bp and 280-bp deletions, respectively, in the genomic DNA of *OsNRAMP1* (Figure S1c). The full transcript of *OsNRAMP1* could not be detected in both *osnramp1-1* and *osnramp1-2* mutants (Figure S1d). Alignment of the corresponding *OsNRAMP1* gene sequences from the mutants and the wild type indicated that deletions in *osnramp1-1* and *osnramp1-2* mutants introduced a premature stop codon within the conserved Nramp domain (pfam01566) critical for OsNRAMP1 function (Figure S1e,f). Together, these results indicate that both *osnramp1-1* and *osnramp1-2* are loss-of-function null alleles. To eliminate the potential off-target mutant, we backcrossed *osnramp1-1* and *osnramp1-2* mutants with wild-type plants and generated a Cas9-free mutant and wild-type pairs for the *OsNRAMP1* gene for subsequent analysis.

Furthermore, *OsNRAMP1*-OE transgenic plants were generated in ZH11 by expressing the *OsNRAMP1* coding sequence under-regulated by the maize *ubiquitin* promoter. Four independent *OsNRAMP1*-OE plants were selected for further analysis. The expression level of *OsNRAMP1* was significantly increased in these *OsNRAMP1*-OE plants (Figure S2a).

To assess the effect of knockout or overexpression of *OsNRAMP1* on other *OsNRAMP* genes, we analysed the expression of five *OsNRAMP* genes in *osnramp1* mutants and *OsNRAMP1*-OE plants. Knockout of *OsNRAMP1* did not affect the expression of other *OsNRAMP* genes, except *OsNRAMP6*, which showed a higher expression in *osnramp1-1* and *osnramp1-2* mutants. In addition, *expression levels of OsNRAMP3* and *OsNRAMP7* were lower in *OsNRAMP1*-OE plants, whereas other *OsNRAMP* genes showed similar expression levels in *OsNRAMP1*-OE plants compared to the wild type (Figure S3).

Field observations of plant growth showed that the leaf colour of transgenic plants was different from that of the wild type at both the tillering and booting stages. At the tillering stage, the leaves of *osnramp1* mutants were yellowish, whereas the leaves of *OsNRAMP1*-OE plants were dark green, compared to green leaves of the wild type (Figure S4a,b). At the booting stage, the *osnramp1* mutants began to show small, reddish-brown lesions or spots in the lower leaves, whereas the *OsNRAMP1*-OE plants and the wild type had normal leaves without lesions or spots (Figure S4d,e). Therefore, the *osnramp1* mutants had decreased chlorophyll (Chl) a and total Chl

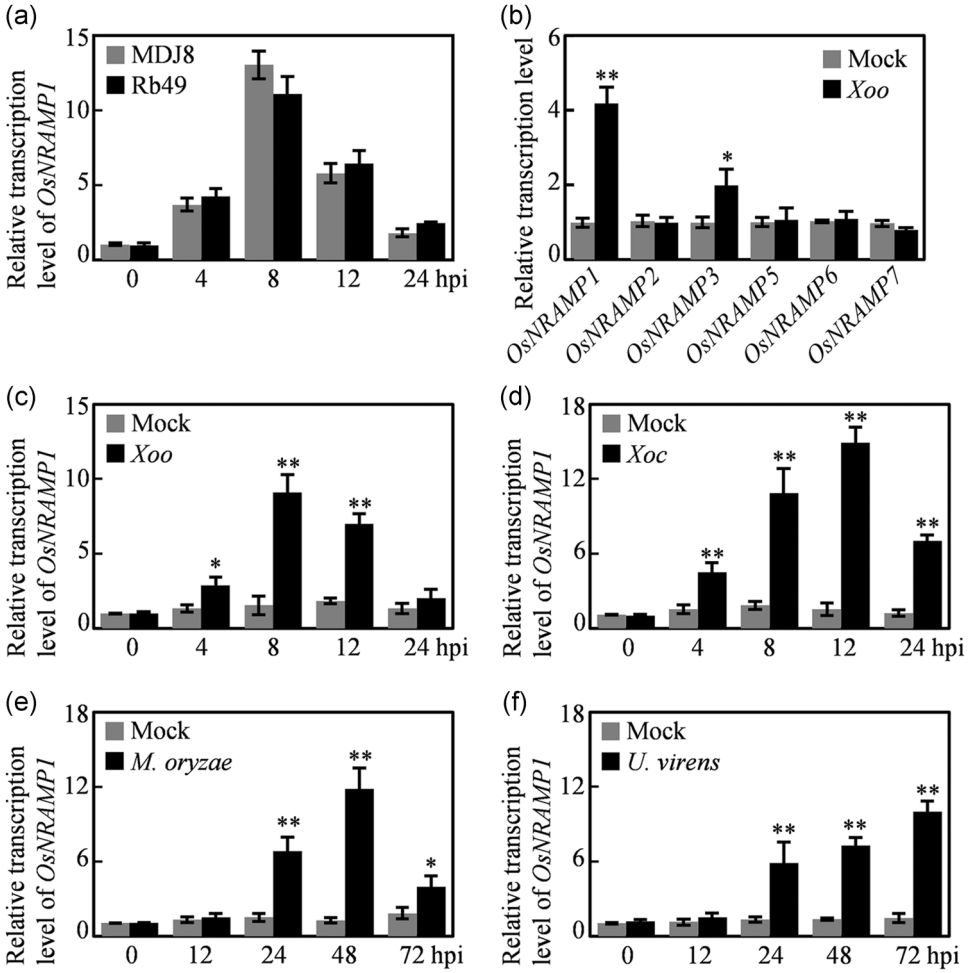


**FIGURE 1** *OsNRAMP1* is activated by different pathogens. (a) Transcriptional level of *OsNRAMP1* in leaves of MDJ8 and Rb49 challenged with *Xoo* PXO61. Rb49, transgenic line carrying the *R* gene *Xa3/Xa26* in the MDJ8 background. (b) Relative transcription levels of six rice *OsNRAMP* genes in leaves of MDJ8 challenged with *Xoo* PXO99 at 12 h. (c) Bacterial pathogen *Xoo* infection activated *OsNRAMP1* expression. Rice leaves were inoculated with *Xoo* strain PXO99 at the booting stage. (d) Bacterial pathogen *Xoc* infection-induced *OsNRAMP1* expression. Rice leaves were inoculated with *Xoc* strain RH3 at the tillering stage. (e) Fungal pathogen *Magnaporthe oryzae infection altered OsNRAMP1 expression*. Rice leaves were inoculated with *M. oryzae* isolate M2 at the tillering stage. (f) Fungal pathogen *Ustilaginoidea virens* infection upregulated OsNRAMP1 expression. Rice panicles were inoculated with *U. virens* isolate WH13 at the booting stage. $H_2O$ inoculation was used for mock treatment. hpi, hours postinfection. Data are means ± SD. Asterisks indicate significant differences between pathogen inoculation and mock treatment determined using a two-tailed Student's *t* test (**$p < 0.01$ or *$p < 0.05$)

contents, and the *OsNRAMP1*-OE plants had increased Chl a and total Chl contents than that of the wild type at both the tillering and booting stages (Figure S4c,f). Furthermore, the *OsNRAMP1*-OE plants matured approximately 32 days later under the long-day condition than the wild type, whereas the *osnramp1* mutants had similar developing stages as the wild type (Figure S4g).

We evaluated disease responses of *osnramp1* mutants and *OsNRAMP1*-OE plants to *Xoo* by inoculation with *Xoo* at the booting stage. The *osnramp1* mutants showed significantly increased resistance to different *Xoo* strains from the Philippines (PXO61, PXO71, PXO99, PXO112, PXO341 PXO347) and China (Zhe173, KS 1-21), with approximately 3.2- to 7-cm shorter lesion lengths than the wild type (Figure 2a,b). The corresponding *Xoo* growth rates in the leaves of *osnramp1-1* plants were 70-fold lower than the wild type at 12 days after *Xoo* inoculation (Figure 2c). However, all the *OsNRAMP1*-OE plants showed comparable lesion length and *Xoo* growth after inoculation with *Xoo* as the wild type (Figure S2b,c). Together, our results of enhanced rice resistance to *Xoo* for *osnramp1* mutants suggest that the *osnramp1* mutation triggers plant immunity.

### 3.3 | The *osnramp1* deletion confers basal resistance to various pathogens in rice

Since *OsNRAMP1* expression was also highly induced by other bacterial and fungal pathogens (Figure 1), we evaluated the role of *OsNRAMP1* in disease resistance to other pathogens such as bacterial pathogen *Xoc* and fungal pathogens *M. oryzae* and *U. virens*. First, we inoculated three *Xoc* strains into the wild type, *osnramp1* mutants and *OsNRAMP1*-OE plants at the tillering stage. The *osnramp1* mutants

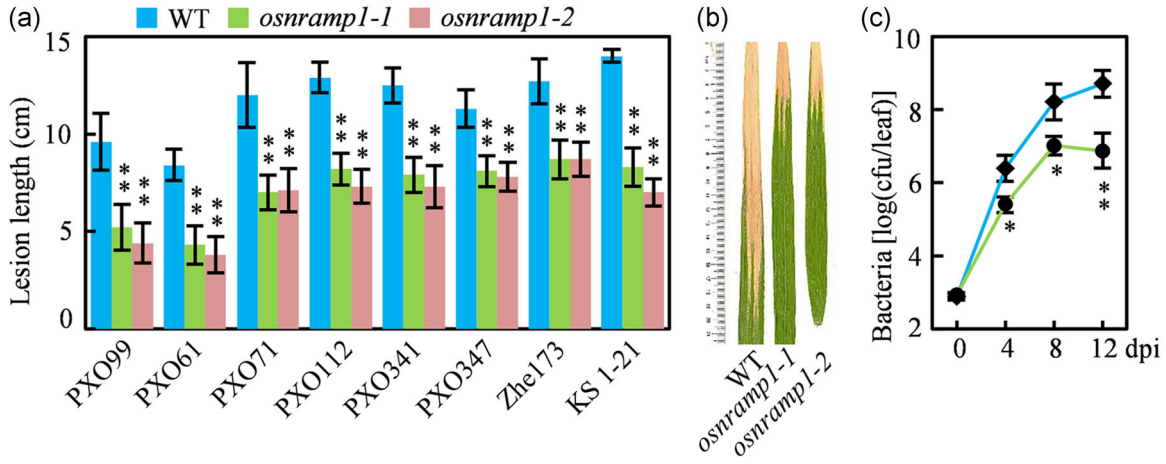


**FIGURE 2** The *osnramp1* mutation triggers rice resistance to *Xoo*. (a) Response of *osnramp1* mutants to different *Xoo* strains. Plants were inoculated with *Xoo* at the booting stage. Each bar represents mean (total 50–70 leaves from 10 plants) ± SD. (b) Phenotype of *osnramp1* mutants after *Xoo* PXO99 infection. (c) Growth of *Xoo* PXO99 in leaves of *osnramp1* mutants. dpi, days postinfection. Data are means ± SD. Asterisks indicate significant differences between the wild type (WT) and *osnramp1* mutants determined using a two-tailed Student's *t* test (**$p < 0.01$ or *$p < 0.05$)

showed enhanced resistance to three *Xoc* strains (RH3, GX01 and HNB8-47), with nearly 36% to 59% decreased lesion length (Figure 3a). In addition, the growth rate of *Xoc* was much lower in the *osnramp1-1* mutant compared to that in the wild type (Figure 3b). However, all the *OsNRAMP1*-OE plants showed comparable lesion length and *Xoc* growth as the wild-type plants after *Xoc* inoculation (Figure S5a,b). Next, *osnramp1* mutants and *OsNRAMP1*-OE plants were punch-inoculated with two *M. oryzae* isolates using the wild type as a control at the tillering stage. The two *osnramp1* mutants showed resistance to *M. oryzae*, with approximately 30%–45% decreased lesion length compared to the wild type (Figure 3c). Consistently, the *osnramp1* mutants had about 48% reduced fungal biomass than the wild type (Figure 3d). In addition, we inoculated *osnramp1* mutants, *OsNRAMP1*-OE plants and the wild type with *U. virens* at the booting stage. The *osnramp1* mutants had approximately seven to nine false smut balls per panicle, whereas the wild type had over eleven false smut balls per panicle (Figure 3e). The corresponding fungal biomass of *U. virens* in florets of *osnramp1* mutants was significantly lower than that in the wild type (Figure 3f). However, the *OsNRAMP1*-OE plants had similar lesion length as the wild type after inoculation with *M. oryzae*, and comparable false smut balls per panicle with the wild type after challenge with *U. virens* (Figure S5a). Therefore, these results collectively indicate that the *osnramp1* mutation regulates basal resistance to various pathogens.

### 3.4 | Impaired ROS homoeostasis in *osnramp1* mutants

To uncover the underlying mechanism of *OsNRAMP1* for basal resistance to bacterial and fungal pathogens, we analysed the transcriptome profiles in *osnramp1* mutant and wild-type leaves. A total of 6269 DEGs were identified, 2542 of which were upregulated DEGs, while 3727 were downregulated DEGs, with at least twofold changes and *a p* value cutoff of 0.05 in the *osnramp1* mutant compared with the wild type (Figure S6a,b; Tables S3 and S4). The GO term analysis revealed that enriched GO terms for the biological process and molecular function in Up-DEGs and Down-DEGs were different (Figure S6c,d). The major enriched GO terms for the biological process in Up-DEGs were metal ion transport and photosynthesis, whereas in Down-DEGs, the terms were protein ubiquitination and protein modification. The primary enriched GO term for molecular functions in Up-DEGs was metal ion transmembrane transporter activity, whereas in Down-DEGs, the term was ubiquitin-protein activity. KEGG pathway enrichment analysis showed that the main enriched pathways in Up-DEGs were photosynthesis and metabolic pathways, whereas in Down-DEGs, these were plant-pathogen interaction and biosynthesis of secondary metabolites (Figure S6e,f).

Among the DEGs, 365 DEGs (136 up-DEGs, 229 down-DEGs) were involved in ROS homoeostasis, including oxidation-reduction, oxidoreductase activity and monooxygenase activity (Figure S7a). For example, nine glutaredoxin (GRX) family members (*OsGRX2*, *OsGRX3*, *OsGRX6*, *OsGRX17*, *OsGRX23*, *OsGRX24*, *OsGRX25*, *OsGRX28*, *OsGRX29*) maintaining the cellular redox state and regulating redox-dependent signalling pathways (Garg et al., 2010), three respiratory burst oxidase homologue family members (also called NADPH oxidases, *OsRbohC*, *OsRbohI*, *OsRbohH*) catalysing the production of apoplastic superoxide (Kaur & Pati, 2016), had significantly decreased expressions in the leaves of the *osnramp1* mutant than in the wild type. Conversely, *polyamine oxidases 5* (*OsPAO5*) and *fatty acid 2-hydroxylases 1* (*OsFAH1*), which play roles in $H_2O_2$ generation (Lv et al., 2021; Nagano et al., 2016), had observably increased transcriptions in *osnramp1* mutant leaves (Figure S7b). RT-qPCR assays verified the downregulated or upregulated expression levels of these representative DEGs involved in ROS homoeostasis (Figure 4a).

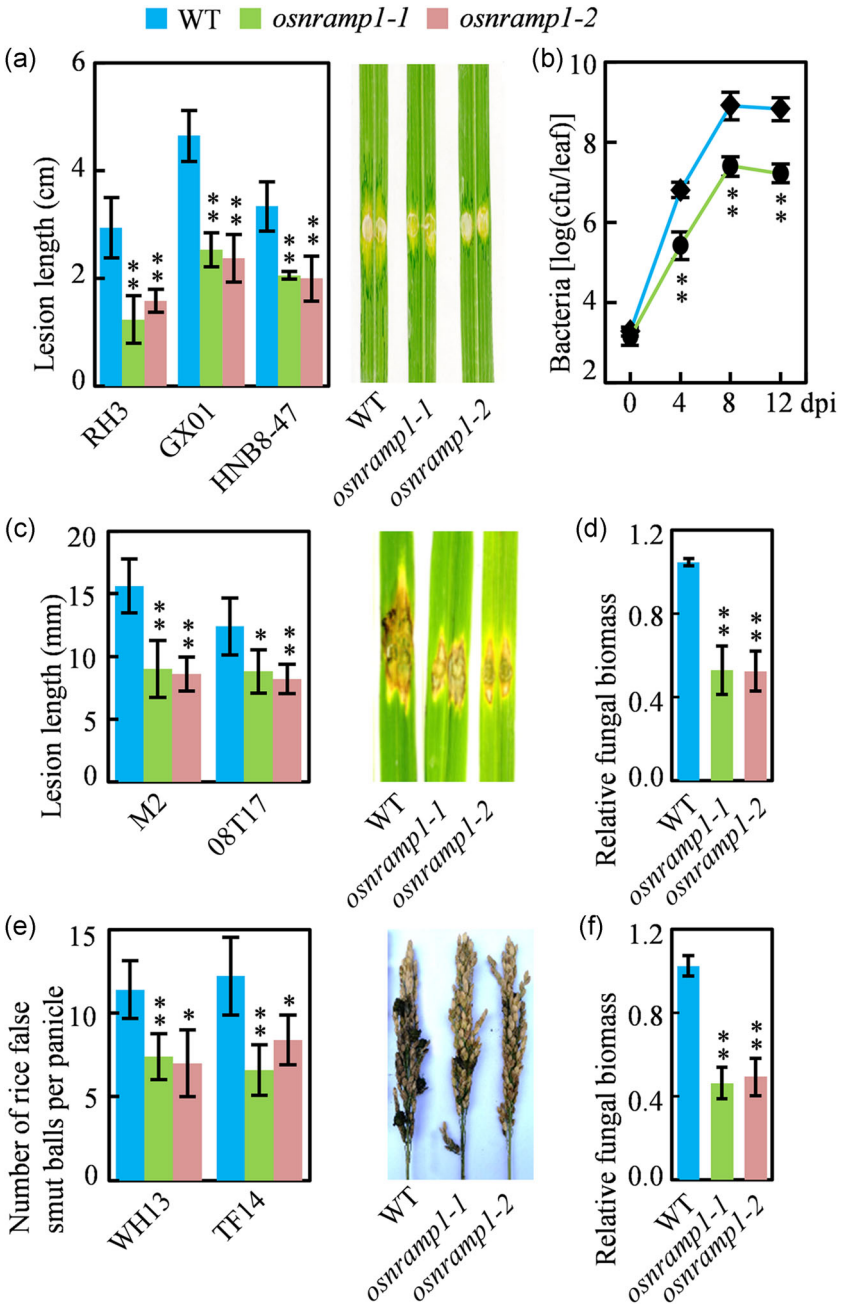


**FIGURE 3** The *osnramp1* deletion confers basal resistance to various pathogens in rice. (a) Response of *osnramp1* mutants to different *Xoc* strains. Plants were inoculated with *Xoc* at the tillering stage. Each bar represents mean (total 30–50 leaves from 10 plants) ± SD. (b) Growth of *Xoc* RH3 in leaves of *osnramp1* mutants. dpi, days postinfection. (c) Response of *osnramp1* mutants to different *Magnaporthe oryzae* isolates. Plants were inoculated with *M. oryzae* at the tillering stage. Each bar represents mean (total 30–50 leaves from 10 plants) ± SD. (d) Relative fungal biomass of *M. oryzae* M2 in the leaves of *osnramp1* mutants. (e) Response of *osnramp1* mutants to different *Ustilaginoidea virens* isolates. Plants were inoculated with *U. virens* at the booting stage. Each bar represents mean (total 50–80 panicles from 10 plants) ± SD. (f) Relative fungal biomass of *U. virens* WH13 in florets of *osnramp1* mutants. Asterisks indicate significant differences between the wild type (WT) and *osnramp1* mutants determined using a two-tailed Student's *t* test (**$p < 0.01$ or *$p < 0.05$) [Color figure can be viewed at wileyonlinelibrary.com]

As *osnramp1* mutants developed lesions or spots on their leaves, we hypothesized that *OsNRAMP1* could regulate resistance of rice to pathogens by altering ROS homoeostasis. Thus, we stained leaves of *osnramp1* mutants, *OsNRAMP1*-OE plants and the wild type with DAB, which is widely used to indicate the accumulation of $H_2O_2$. DAB staining showed that the apparent red-brown precipitate was exclusively observed in *osnramp1* mutant leaves, whereas no such precipitate was observed in *OsNRAMP1*-OE plants and wild-type leaves (Figure 4b). Consistently, the $H_2O_2$ content was 1.5-fold higher in *osnramp1* mutants than in *OsNRAMP1*-OE plants and the wild-type (Figure 4c). A higher $H_2O_2$ content was also detected in panicles of the *osnramp1* mutants than in *OsNRAMP1*-OE plants or the wild type (Figure S8a).

The abundance of $H_2O_2$ implied the disrupted ROS scavenging system in the *osnramp1* mutant. To test the possibility, we measured the activities of two major antioxidative enzymes, SOD and catalase (CAT), which catalyse superoxide anion radical disproportionation to $H_2O_2$ and the decomposition of $H_2O_2$, respectively, in both the leaves and panicles of these plants (Miller et al., 2010). The SOD activity was significantly higher in *osnramp1* mutants than that in *OsNRAMP1*-OE plants and the wild type both in leaves and panicles. In contrast, the CAT activity was observably lower in *osnramp1* mutants, while only slightly greater in the *OsNRAMP1*-OE2 plant than that of the wild type in the leaves and panicles (Figure 4d and S8b). The higher SOD activity and the lower CAT activity were consistent with more $H_2O_2$ accumulation in *osnramp1* mutants than that in the

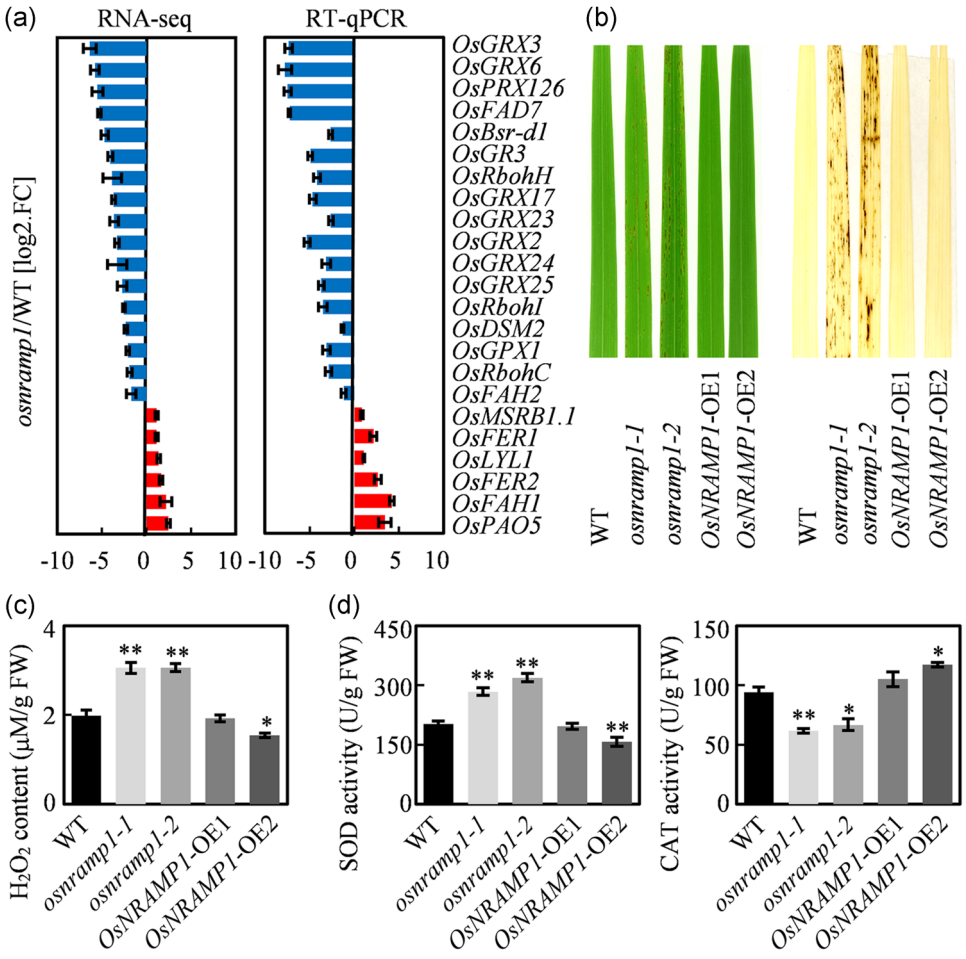


**FIGURE 4** Impaired reactive oxygen species homoeostasis in *osnramp1* mutants. (a) Quantitative real-time polymerase chain reaction (RT-qPCR) validation of representative DEGs derived by RNA-seq analysis. (b) 3,3′-diaminobenzidine (DAB) staining for $H_2O_2$ accumulation in the leaves of *osnramp1* mutants, *OsNRAMP1*-OE plants and the wild type (WT). (c) $H_2O_2$ content in the leaves of *osnramp1* mutants, *OsNRAMP1*-OE plants and the wild type. (d) Superoxide dismutase (SOD) and catalase (CAT) activities in the leaves of *osnramp1* mutants, *OsNRAMP1*-OE plants and the wild type. Data are means ± SEM. Asterisks indicate significant differences between the wild type and *osnramp1* mutants or *OsNRAMP1*-OE plants determined using a two-tailed Student's *t* test (**$p < 0.01$ or *$p < 0.05$) [Color figure can be viewed at wileyonlinelibrary.com]

wild type. Taken together, the results suggest that accumulated $H_2O_2$ possibly results in enhanced basal resistance to different pathogens in *osnramp1* mutants.

## 3.5 | ROS production in *osnramp1* mutants upon PAMP treatment

PAMPs, bacterial flg22 and fungal chitin, have been shown to trigger ROS burst in rice. To examine whether *OsNRAMP1* affects ROS production in response to PAMP treatment, we measured ROS accumulation in the leaves of *osnramp1* mutants and *OsNRAMP1*-OE plants with the wild type as a control upon flg22 and chitin treatments. Both flg22- and chitin-triggered ROS bursts were greater in *osnramp1* mutants than in the wild type (Figure 5). In contrast, the PAMPs-induced ROS burst was less in *OsNRAMP1*-OE plants than in the wild type (Figure 5). These results indicate that *OsNRAMP1* might regulate the ROS burst during PAMP-triggered immune responses in rice.

## 3.6 | Altered metal ion homoeostasis in *osnramp1* mutants

OsNRAMP1 has been reported to function as an iron transporter, which can transport Fe, Cd, Mn and As in heterologous yeast (Chang et al., 2020; Takahashi et al., 2011; Tiwari et al., 2014), and contribute to the uptake of Mn and Cd in rice (Chang et al., 2020; Takahashi et al., 2011). Therefore, we analysed the metal ion content in the leaves of *osnramp1* mutants, *OsNRAMP1*-OE plants and the wild type. Compared to the wild type, *osnramp1* mutants had decreased levels of Cd (−33.1% to 43.3%), Mn (−23.5% to 30.7%), Ni (−31.3% to 46.2%) and Pb (−44.2% to 57.1%), whereas *OsNRAMP1*-OE plants had increased levels of Cd (+46.3% to 50.9%), Mn (+26.3% to 43.5%),

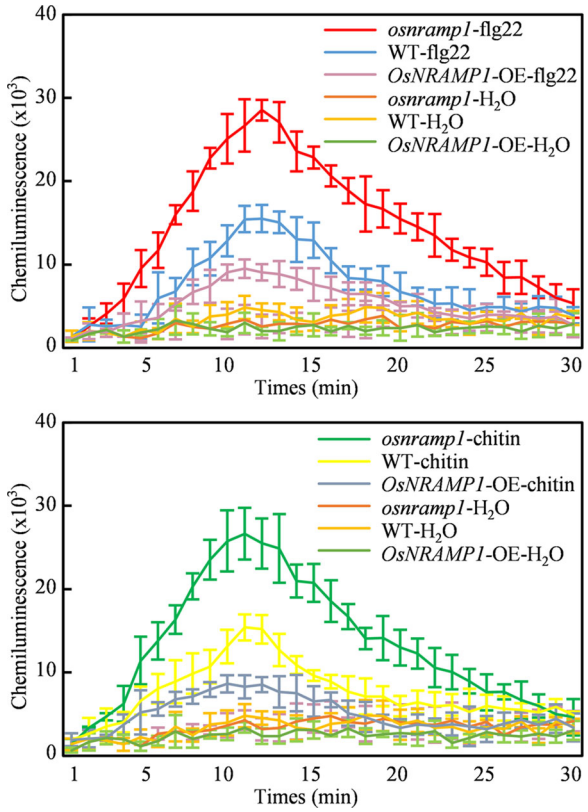


**FIGURE 5** Reactive oxygen species (ROS) accumulation in the leaves of the *osnramp1* mutant, *OsNRAMP1*-OE plants and the wild type (WT) after flg22 and chitin treatments. Rice leaf discs were treated with 10 μM flg22 or 1 μM chitin, with water as a control. Data are means ± SD [Color figure can be viewed at wileyonlinelibrary.com]

Ni (+54.4% to 71.9%) and Pb (+50.1% to 63.6%). Moreover, there were similar contents of As, Cu, Fe, Mg, Mo and Zn in the leaves of the *osnramp1* mutant, *OsNRAMP1*-OE plants and the wild type (Figure S9). Altered levels of Cd and Mn in *osnramp1* mutants and *OsNRAMP1*-OE plants were consistent with previous reports (Chang et al., 2020; Takahashi et al., 2011), further confirming the role of OsNRAMP1 as a Cd and Mn transporter. Interestingly, we further discovered that Ni and Pb levels were also altered in *osnramp1* mutants and *OsNRAMP1*-OE plants.

There were 384 DEGs (163 up-DEGs, 221 down-DEGs) that played a role in metal ion transport or ion binding (Figure S10a). Some metal ion transporter genes that are responsible for metal uptake or transportation had differentially expressed levels (Figures 6a and S10b). For example, *OsCd1* and *OsLCT1*, encoding Cd transporters (Uraguchi et al., 2011; Yan et al., 2019), had decreased expression levels in the *osnramp1* mutant. *OsVIT2*, encoding a vacuolar Fe and Zn transporter that modulates Fe/Zn translocation between leaves and seeds (Zhang et al., 2012), had markedly increased expression in the *osnramp1* mutant. *OsMTP11* and *OsYSL2*, encoding a Mn transporter and a metal–nicotianamine transporter, respectively, being responsible for the long-distance transport of Mn (Ishimaru et al., 2010; G. Ma et al., 2018), had decreased transcription in the *osnramp1* mutant. *OsHMA9*, encoding a metal efflux transporter and playing roles in metal detoxification at higher concentrations of Cu, Zn, Cd and Pb (Lee et al., 2007), had clearly attenuated expression in the leaves of *osnramp1* mutant than the wild type. *OsHAC1;1* and *OsHAC1;2*, functioning as As reductases (S. Shi et al., 2016), showed slightly enhanced expression levels in the *osnramp1* mutant than in the wild type.

We assessed the expressions of some representative metal ion transporters in the leaves of *osnramp1* mutants, *OsNRAMP1*-OE plants and the wild type. *OsLCT1*, *OsYSL2*, *OsMTP11* and *OsHMA9* had markedly decreased expression levels in *osnramp1* mutants, but increased transcriptions in *OsNRAMP1*-OE plants relative to the wild type (Figure 6b). *OsCd1* had markedly decreased transcription in *osnramp1* mutants, but comparable expression in *OsNRAMP1*-OE plants than in the wild type. In contrast, *OsHAC1;2* had increased expression in *osnramp1* mutants, but decreased expression in *OsNRAMP1*-OE plants than in the wild type (Figure 6b). These different expression patterns of metal ion transporters in *osnramp1* mutants or *OsNRAMP1*-OE plants further suggest that OsNRAMP1 may regulate metal ion homoeostasis through its transportation activities directly and transcription regulation of other metal transporters indirectly in rice.

## 3.7 | Modified metal ion-dependent enzyme activities

Mn acts as an essential co-factor of hundreds of metalloenzymes in plants, playing important roles in a broad range of Mn-dependent enzyme-catalysed reactions, including redox reactions and ROS scavenging (Alejandro et al., 2020). Under conditions of Mn deficiency, plant leaves may develop brownish or necrotic spots due to the decreased Mn-SOD activity (Broadley et al., 2012). Thus, we measured the Mn-SOD activity in rice leaves, and the results indicated that the Mn-SOD activity was evidently lower in *osnramp1* mutants, but only slightly higher in the *OsNRAMP1*-OE2 plant than the wild type (Figure 7a). Lower Mn-SOD activity was also obtained in the panicle of *osnramp1* mutants (Figure S8b). In addition, the expression level of *OsMSD* encoding Mn-SOD was significantly lower in *osnramp1* mutants relative to that in the wild type (Figure 7b).

Except for Mn-SOD, we simultaneously assessed the activities of Cu/Zn-SOD and Fe-SOD, which use Cu or Zn and Fe as co-factors, respectively. The *osnramp1* mutants had higher Cu/Zn-SOD and Fe-SOD activities than that of the wild type in both leaves and panicles (Figures 7a and S8b). We simultaneously determined the transcription levels of four *OsCSD* genes encoding Cu/Zn-SOD and two *OsFSD* genes encoding Fe-SOD (J. Li, Cao, et al., 2019; Y. Li, Wang et al., 2019). *OsCSD3* and *OsCSD4* showed markedly increased expressions in *osnramp1* mutants, whereas *OsCSD3* showed decreased transcription in *OsNRAMP1*-OE plants. *OsCSD1* and *OsCSD2* had comparable expressions in *osnramp1* mutants and *OsNRAMP1*-OE plants than in the wild type (Figure 7b). Two *OsFSD* genes had similar levels in both the *osnramp1* mutant and t he*OsNRAMP1*-OE plant as that in the wild type (Figure 7b). Considering the similar levels of Cu

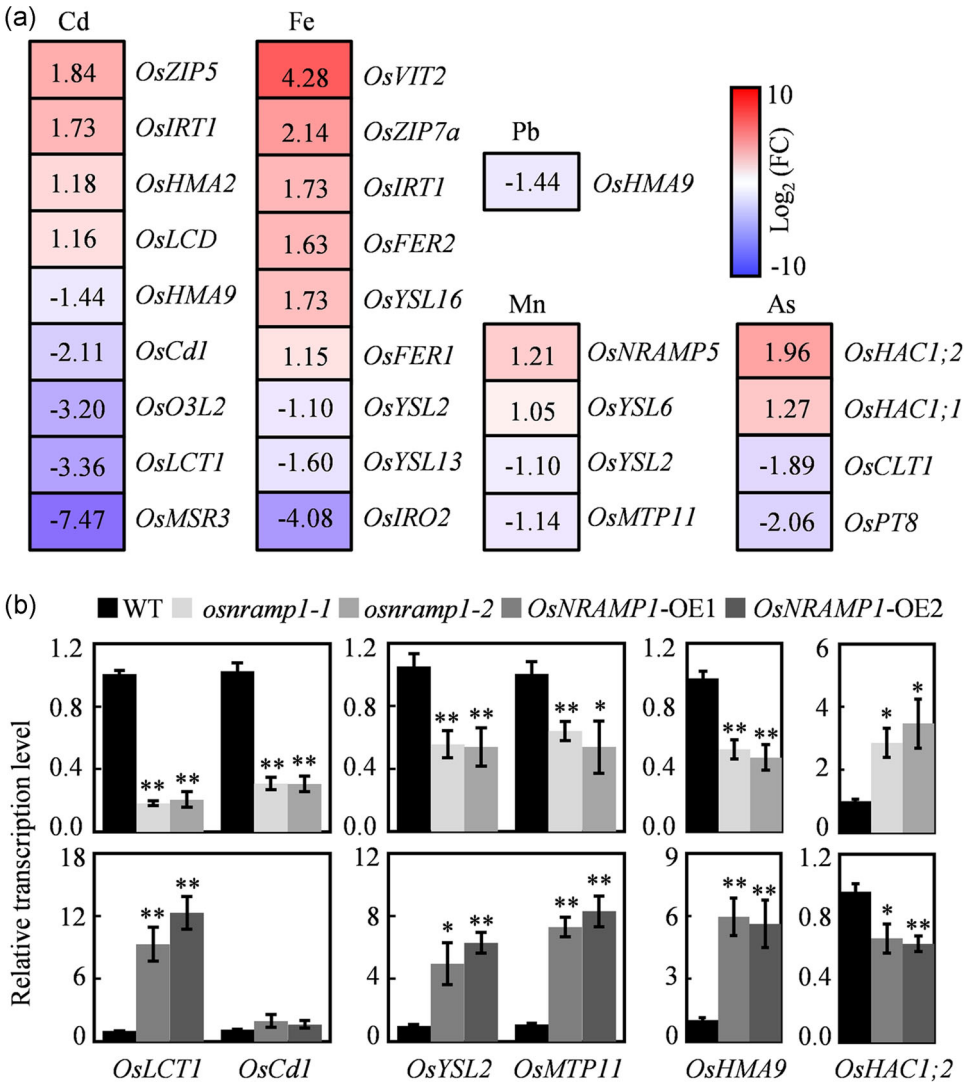


**FIGURE 6** Altered expression levels of metal transporters or metal-related genes in *osnramp1* mutants. (a) Heat map of differentially expressed genes involving in uptake or transport for Cd, Fe, Mn, As and Pb. The number indicates the value ($Log_2$) of gene expression for *osnramp1* mutant relative to that for the wild type (WT). (b) Expression levels of representative metal transporter genes in the leaves of *osnramp1* mutants, *OsNRAMP1*-OE plants and the wild type. Data are means ± SD. Asterisks indicate significant differences between the wild type and *osnramp1* mutants or *OsNRAMP1*-OE plants determined using a two-tailed Student's *t* test (**$p < 0.01$ or *$p < 0.05$) [Color figure can be viewed at wileyonlinelibrary.com]

and Zn in *osnramp1* mutants, the increased *OsCSD3* and *OsCSD4* expression probably contributed to enhanced Cu/Zn-SOD activity in the *osnramp1* mutant.

In addition, we analysed the expressions of *OsCatA*, *OsCatB* and *OsCatC*, which encode catalase (CAT) involved in the degradation of $H_2O_2$ into water and oxygen. There were significantly lower expressions of *OsCatA* and *OsCatB* in *osnramp1* mutants, but higher expressions of these in *OsNRAMP1*-OE plants. *OsCatC* expression was lower in *OsNRAMP1*-OE plants, but similar in *osnramp1* mutants compared to that in the wild type (Figure 7b). Since Mn and Fe have been identified as cofactors for catalase (Yocum & Pecoraro, 1999), both decreased expression of *OsCat* genes and compromised Mn accumulation together lead to attenuated CAT activity in *osnramp1* mutants (Figure 4d). Collectively, these results indicate that both insufficient metal accumulation and lower expression levels of ROS-scavenging enzymes cause altered metal-dependent enzyme activity, resulting in $H_2O_2$ accumulation in *osnramp1* mutants.

## 3.8 | Altered ROS homoeostasis may contribute to disease resistance

GRXs are ubiquitous oxidoreductase enzymes that play critical roles in oxidative stress response and redox regulation. Plants usually use multiple strategies including GRXs to protect themselves from the damage of accumulation of ROS under oxidative stress by scavenging ROS (Rouhier et al., 2008). Here, we found that the expression of nine *GRX* genes, which encode plant-specific CC-type GRX and have been

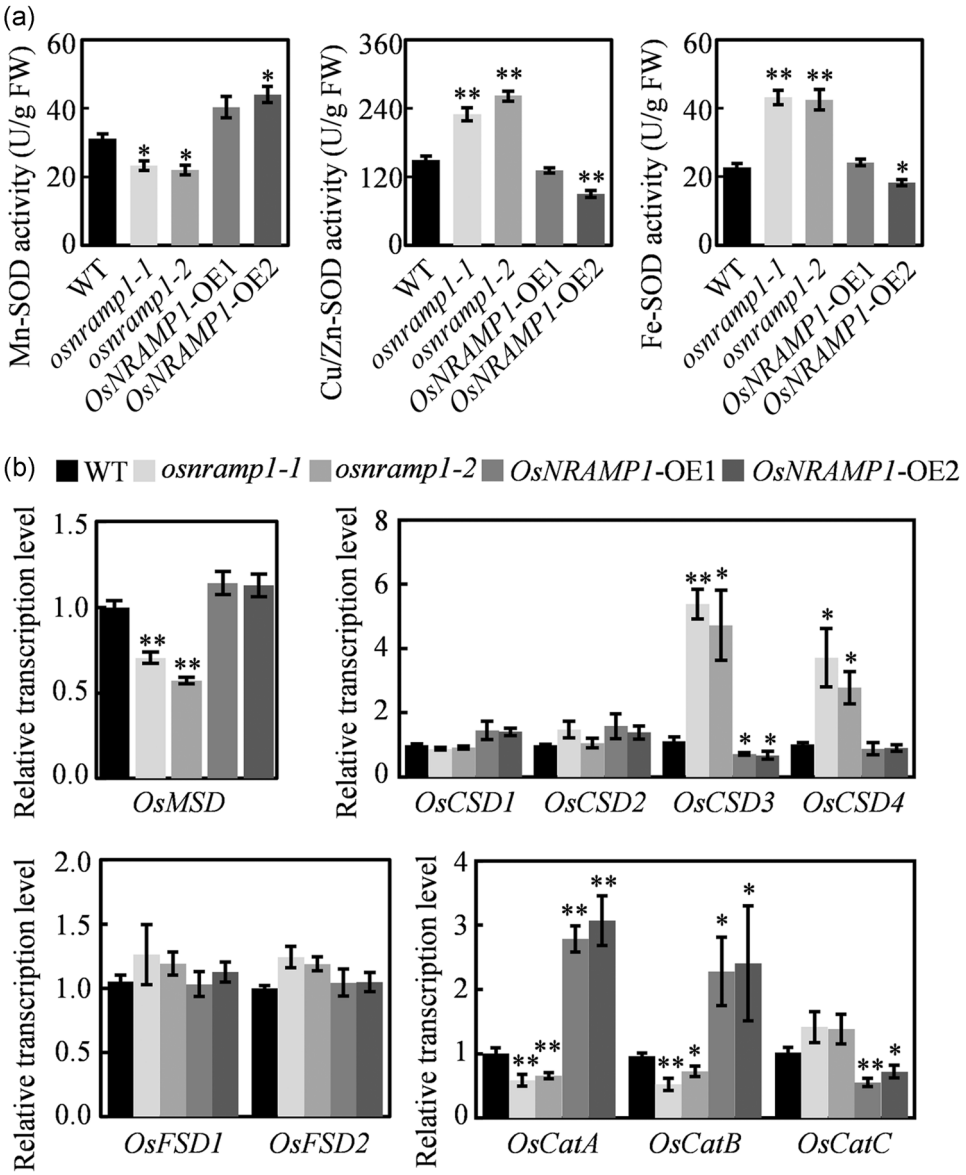


**FIGURE 7** Impaired metal-dependent enzyme activity and gene expression in *osnramp1* mutants. (a) Mn-superoxide dismutase (SOD), Cu/Zn-SOD and Fe-SOD activities in the leaves of *osnramp1* mutants, *OsNRAMP1*-OE plants and the wild type (WT). Data are means ± SEM. (b) Expression levels of *OsMSD*, *OsCSD*, *OsFSD* and *OsCat* genes in the leaves of *osnramp1* mutants, *OsNRAMP1*-OE plants and the wild type. Data are means ± SD. Asterisks indicate significant differences between the wild type and *osnramp1* mutants or *OsNRAMP1*-OE plants determined using a two-tailed Student's *t* test (**$p < 0.01$ or *$p < 0.05$)

reported to be repressed in response to $H_2O_2$ stress (Garg et al., 2010), was markedly decreased in *osnramp1* mutants (Figure 4a). Subsequently, we analysed the GRX activity; about 42.6% to 46.8% loss of GRX activity was observed in *osnramp1* mutants relative to the wild type (Figure 8a). These results suggest that GRX-mediated ROS scavenging was greatly compromised in *osnramp1* mutants.

Since GRXs are glutathione (GSH)-dependent redox enzymes that catalyse the reduction of disulphides through reduced GSH in a coupled system with NADPH and glutathione reductase, we therefore analysed the concentrations of GSH (reduced state of glutathione) and GSSG (oxidized state of glutathione) in the leaves of *osnramp1* mutants and *OsNRAMP1*-OE plants along with the wild type. Relatively lower GSH and higher GSSG concentrations were observed in *osnramp1* mutants compared to the wild type, thus leading to a decrease of the GSH/GSSG ratio. In contrast, higher GSH and lower GSSG concentrations were found only in *OsNRAMP1*-OE2 plants along with an increase of the GSH/GSSG ratio (Figure 8b). We also analysed the concentration of NADPH, which provides reducing power and is essential for the proper scavenging of ROS in plant cells. The ratio of NADPH/$NADP^+$ (reduced state/oxidized state) is calculated as a proxy for reducing power of NADPH (Liu et al., 2018). Lower NADPH and higher $NADP^+$ concentrations were detected in *osnramp1* mutants compared to that in the wild type, resulting in a decrease of the NADPH/$NADP^+$ ratio. However, higher NADPH and

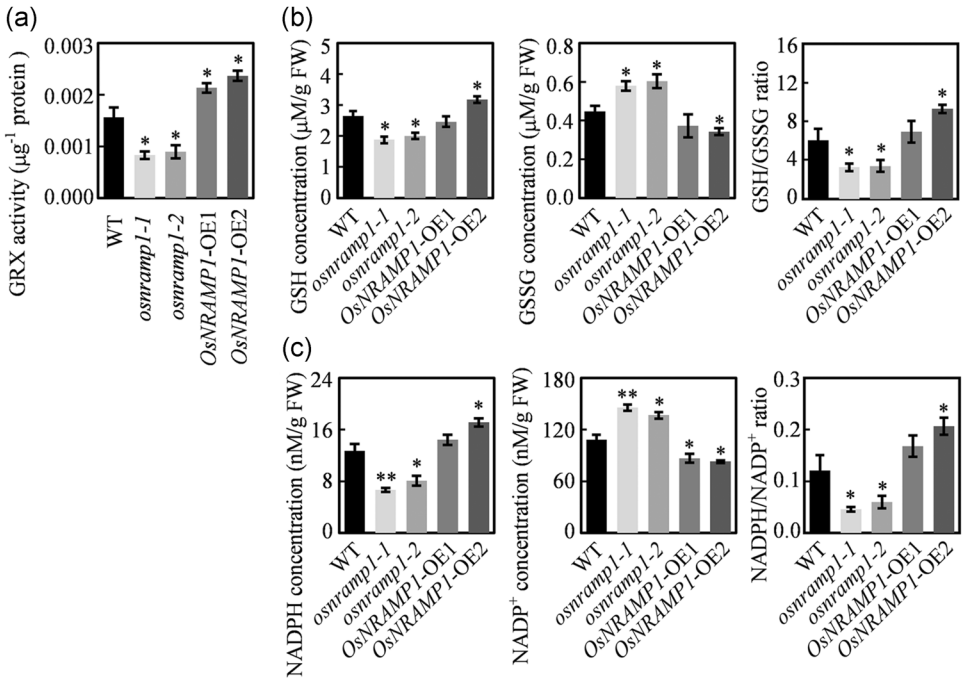


**FIGURE 8** Altered reactive oxygen species homoeostasis in *osnramp1* mutants. (a) Glutaredoxin (GRX) activity in the leaves of *osnramp1* mutants, *OsNRAMP1*-OE plants and the wild type (WT). (b) Analysis of GSH and GSSG activities and the GSH/GSSG ratio in the leaves of *osnramp1* mutants, *OsNRAMP1*-OE plants and the wild type. (c) Analysis of NADPH and $NADP^+$ activities and the NADPH/$NADP^+$ ratio in the leaves of *osnramp1* mutants, *OsNRAMP1*-OE plants and the wild type. Data are means ± SEM. Asterisks indicate significant differences between the wild type and *osnramp1* mutants or *OsNRAMP1*-OE plants determined using a two-tailed Student's *t* test (**$p < 0.01$ or *$p < 0.05$)

lower $NADP^+$ contents were detected in *OsNRAMP1*-OE plants along with an increase of the NADPH/$NADP^+$ ratio (Figure 8c). These results suggest that the reducing power of GSH and NADPH may also contribute to unbalanced ROS homoeostasis, resulting in enhanced resistance against various pathogens in *osnramp1* mutants.

### 3.9 | Agronomic traits of *osnramp1* mutants

To further investigate the effect of *OsNRAMP1* on metal ion accumulation in rice grain, *osnramp1* mutants, *OsNRAMP1*-OE plants and the wild type were grown in the paddy field of the experimental farm on campus. Compared to the wild type, the contents of Cd, Mn, Ni and Pb in the grains of *osnramp1* mutants decreased 40.2%–47.8%, 17.1%–22.8%, 35.8%–36.1% and 25.3%–26.1%, respectively. In contrast, the concentrations of Cd, Mn, Ni and Pb in the grains of *OsNRAMP1*-OE plants increased 57.3%–65.1%, 20.6%–22.8%, 61.2%–68.0% and 45.9%–59.6%, respectively, compared to those of the wild type. Moreover, there were similar contents of As, Cu, Fe, Mg, Mo and Zn in the grains of the *osnramp1* mutant, *OsNRAMP1*-OE plants and the wild type (Figure 9a).

In addition, to assess the effect of *OsNRAMP1* on rice growth and development, we examined a number of agronomic traits of these plants. The *osnramp1* mutants had similar agronomic traits including tiller number, flag leaf length, flag leaf width, grain length and grain width as wild type, but had slightly decreased panicle length (−2.5% to 6.7%), grain number per panicle (−6.3% to 7.2%), seed setting rate (−3.9% to 4.4%), 1000-grain weight (−3.5% to 4.3%) and yield per plant (−4.6% to 4.9%). However, the *OsNRAMP1*-OE plants showed significantly decreased flag leaf length (−26.3% to 27.4%), flag leaf width (−30.6% to 32.5%), panicle length (−8.1% to 13.1%), grain number per panicle (−13.1% to 16.7%), seed setting rate (−18.8% to 19.1%), 1000-grain weight (−4.8% to 8.1%) and yield per plant (−14.7% to 18.3%), but increased tiller number (+35.4% to 51.5%), compared with the wild type (Figure 9b). These results suggest that knockout of *OsNRAMP1* has minor adverse effects on agronomic traits, whereas overexpression of *OsNRAMP1* severely restrains agronomic traits.

## 4 | DISCUSSION

Previous results have uncovered the roles of OsNRAMP1 in metal ion transportation (Chang et al., 2020; Takahashi et al., 2011; Tiwari et al., 2014). In this study, we uncover the novel function of *OsNRAMP1* in plant immunity via the regulation of ROS homoeostasis.

### 4.1 | OsNRAMP1 acts as a multiple metal ion transporter

NRAMP proteins function as divalent metal transporters in a wide range of living beings from bacteria to humans (Bozzi & Gaudet, 2021).

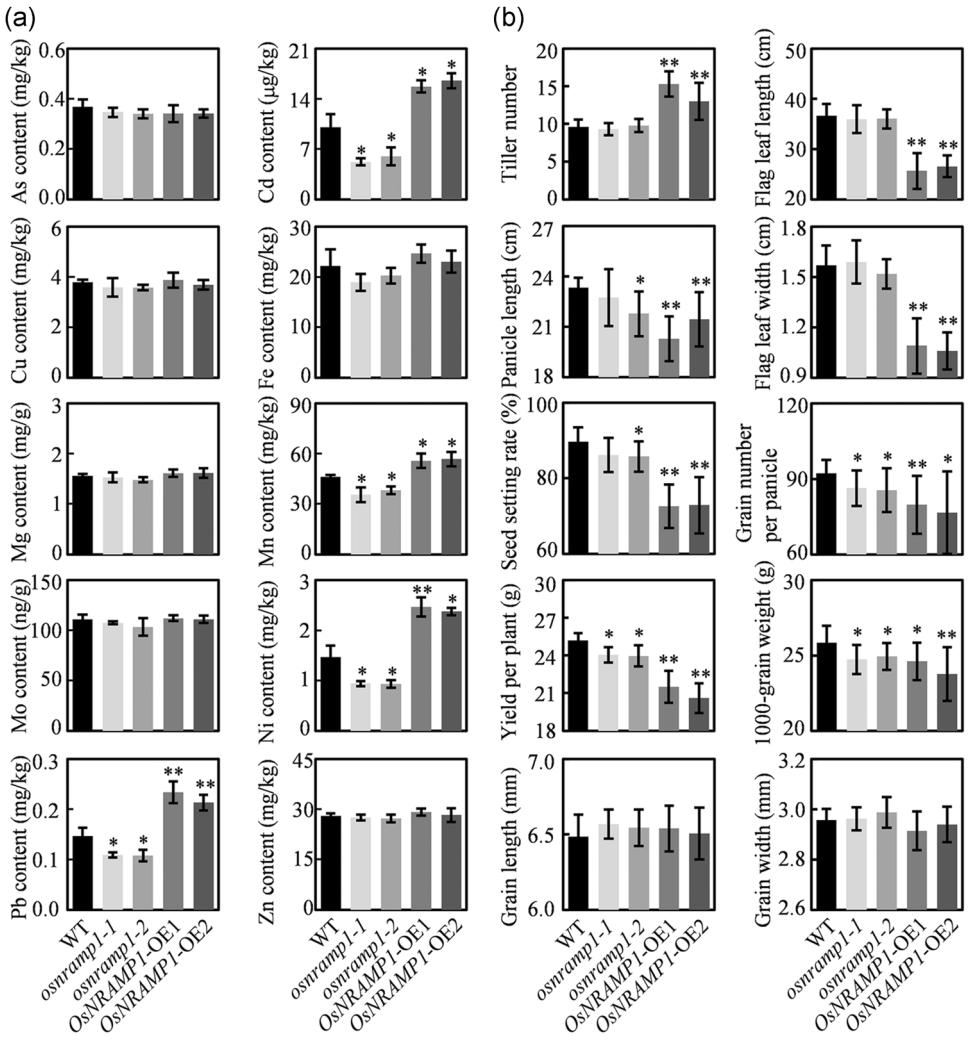


**FIGURE 9** Agronomic traits and element concentrations in the grains of *osnramp1* mutants, *OsNRAMP1*-OE plants and the wild type (WT) grown in the field. (a) Elemental concentrations in the grains of *osnramp1* mutants, *OsNRAMP1*-OE plants and the wild type. (b) Agronomic traits of *osnramp1* mutants, *OsNRAMP1*-OE plants and the wild type. Data are means ± SD. Asterisks indicate significant differences between the wild type and *osnramp1* mutants or *OsNRAMP1*-OE plants determined using a two-tailed Student's *t* test (**$p < 0.01$ or *$p < 0.05$)

A large number of NRAMP proteins of different species have been reported as metal ion transporters mediating multiple-element transportation. For example, rat DCT1/NRAMP2 has a broad substrate including Fe, Zn, Mn, Co, Cd, Cu, Ni and Pb (Gunshin et al., 1997). Plant NRAMP proteins have been reported for transporters of Fe, Mn, Cd, Zn and Ni (Bozzi & Gaudet, 2021). Although OsNRAMP1 has been reported to transport several ions including Fe, Cd, Mn and As in heterologous expression systems using yeast (Chang et al., 2020; Takahashi et al., 2011; Tiwari et al., 2014), it has been experimentally validated to contribute to the uptake of Mn and Cd in rice roots and the accumulation of Mn and Cd in rice shoots or grains (Chang et al., 2020; Takahashi et al., 2011). Our study verified that OsNRAMP1 could transport Mn and Cd in rice, consistent with previous reports. In addition, we demonstrated that OsNRAMP1 could also transport Ni and Pb in rice. The knockout of *OsNRAMP1* plants led to significantly lower Cd, Mn, Ni and Pb concentrations, whereas overexpression of *OsNRAMP1* plants led to higher Cd, Mn, Ni and Pb concentrations than that in the wild type in both leaves and grains (Figures 9a and S9). Furthermore, the decreased chlorophyll content of *osnramp1* mutants was possibly correlated with insufficient metal ions such as Mn (Figure S4). However, additional in vitro and in vivo assays should be carried out to verify the transportation activity of OsNRAMP1 on Ni and Pb in the future. Collectively, combining published results and the present data, it is likely that OsNRAMP1 has a broad spectrum of metal cation substrates.

NRAMP proteins of a species usually have diverse transport activities on metal ions. *Arabidopsis* harbours six NRAMP proteins; each of them uptakes different metal ions. AtNRAMP1 and AtNRAMP2 can transport Mn (Curie et al., 2000), AtNRAMP3 and AtNRAMP4 show transport activity on Fe, Mn and Cd (Lanquar et al., 2005; Thomine et al., 2003), whereas AtNRAMP6 mediates uptake of Fe and Cd (Cailliatte et al., 2009; J. Li, Wang, et al., 2019; Y. Li, Cao, 2019). Similarly, seven rice NRAMP proteins have diverse metal-ion preferences. OsNRAMP2, OsNRAMP3 and OsNRAMP4

are involved in the transportation of Fe, Mn and Al, respectively (J. Y. Li et al., 2014; Y. Li et al., 2021; Yamaji et al., 2013). OsNRAMP5 is a major influx transporter for Mn, Fe and Cd (Sasaki et al., 2012). OsNRAMP6 is involved in the uptake of Fe and Mn (Peris-Peris et al., 2017). OsNRAMP1 mediates the uptake of Cd, Mn, Ni and Pb, indicating that OsNRAMP1 has different transport activities on metal ions compared with other OsNRAMP proteins. NRAMP proteins have different substrate preferences on metal ions that possibly rely on their diverse active amino acid residues, which determine the binding affinity with different metal cations (Bozzi & Gaudet, 2021). Therefore, resolving the crystal structure of OsNRAMP1 may provide direct evidence for its multiple metal ion transportation activity.

The contents of Cd, Mn, Ni and Pb were decreased in *osnramp1* mutants, whereas the expressions of many metal transporters were upregulated or downregulated (Figures 6a and S10). The reprogrammed transcription of these metal transporters may be attributable to deficiency of some metal ions in transgenic plants. Further measurement of metal ions in specific organelles may directly support the altered expression levels of these metal transporters because their functions are limited to specific organelles and are responsible for sufficiency or deficiency of different metals.

## 4.2 | The *osnramp1* mutation regulates basal resistance to various pathogens in rice

Several *NRAMP* genes have been reported to positively or negatively regulate resistance to different pathogens in animals and plants. Mice lacking functional *NRAMP1* were susceptible to viral, bacterial and protozoan pathogens (Blackwell et al., 2001). The *Arabidopsis atnramp3* mutant showed increased susceptibility to *Erwinia chrysanthemi*, whereas the *AtNRAMP3*-overexpressing plants showed resistance to infection by *E. chrysanthemi* (Segond et al., 2009). Conversely, *Drosophila* dNRAMP and mammalian NRAMP2 were required for Sindbis virus infection, acting as cellular receptors for the Sindbis virus; the loss of function of *Drosophila dNRAMP* enhanced resistance against Sindbis virus (Rose et al., 2011). The loss of function of rice *OsNRAMP6* conferred enhanced resistance against blast fungus (Peris-Peris et al., 2017). We found upregulation of *OsNRAMP1* in leaves infected with bacterial pathogens *Xoo* and *Xoc*, or fungal pathogen *M. oryzae*, and in panicles infected with fungal pathogen *U. virens* (Figure 1). Correspondingly, the lack of functional *OsNRAMP1* resulted in enhanced resistance to these bacterial pathogens and fungal pathogens, suggesting that the *osnramp1* mutation triggers immunity of rice against pathogen infection (Figures 2 and 3). Although the expression of *OsNRAMP6* was increased in *osnramp1* mutants, *OsNRAMP6* negatively regulated resistance of rice to *M. oryzae* (Peris-Peris et al., 2017). Therefore, we conjectured that the enhanced resistance to different pathogens for the *osnramp1* mutants was due to the deletion of *OsNRAMP1*, while not increasing the expression of *OsNRAMP6*. Overall, we speculate that *NRAMP* genes from different species play diverse roles upon pathogen infection.

The deficiency of Mn and attenuated expression of *OsMSD* and *OsCats* could jointly weaken Mn-dependent metalloenzyme activity including Mn-SOD and CAT, which synergistically affect Mn-dependent enzyme-catalysed reactions in the *osnramp1* mutant (Alejandro et al., 2020). The subcellular localization of these enzymes is variable as mitochondrial localization of Mn-SOD, peroxisome and cytoplasm localization of Cu/Zn-SOD, and chloroplast localization of Fe-SOD. Although there were unchanged levels of total Cu, Zn and Fe in the leaves and grains of *osnramp1* mutants (Figures 9a and S9), a number of DEGs were involved in transportation or homoeostasis of Cu, Zn and Fe (Figure S10b). Importantly, we could not quantify the concentrations of Cu, Zn and Fe in different rice organelles, and could not quantify $Fe^{2+}$ or $Fe^{3+}$ due to technical limitations. Further, the expressions of *OsCSDs* were increased in *osnramp1* mutants (Figure 7). These may cause higher Cu/Zn-SOD and Fe-SOD activities in *osnramp1* mutants (Figures 7 and S8). Although a lower Mn-SOD level and higher Cu/Zn-SOD and Fe-SOD contents were found, the total SOD activity was increased in the *osnramp1* mutant. Therefore, we presumed that increased SOD activity and decreased CAT activity potentially contribute to the accumulation of $H_2O_2$, leading to enhanced resistance to various pathogens of *osnramp1* mutants. A similar result was also observed in the *Arabidopsis atnramp3atnramp4* double mutant, which showed reduced levels of ROS and increased susceptibility to *E. chrysanthemi* (Segond et al., 2009). Apart from Mn, Fe is also an essential co-factor for diverse metalloenzymes in plants, including Fe-SOD and CAT. Therefore, we could not exclude the possibility that the Fe-dependent enzymes may play a role in acting against pathogens for the *osnramp1* mutant, as OsNRAMP1 has also been previously reported to be an Fe transporter (Takahashi et al., 2011). Collectively, we speculate that altered Cu-, Zn- or Fe-dependent enzymes reprogramme their catalysed reactions including SOD- and CAT-involved $H_2O_2$ metabolism. In addition, altered expressions of metal ion-dependent enzyme genes and lower levels of cations together cause the accumulation of $H_2O_2$, which confers basal resistance of *osnramp1* mutants to bacterial and fungal pathogens. Based on these data, we propose a working model to explain how OsNRAMP1 promotes metal ion transportation and plant immunity. OsNRAMP1 acts as a multiple metal ion transporter that transports Mn, Ni, Cd and Pb in rice. Knockout of *OsNRAMP1* decreases the contents of these metal ions and reprogrammes metal ion-dependent enzyme activity, causing $H_2O_2$ accumulation, thereby triggering basal immunity (Figure 10).

In contrast, there were abundant Mn and increased expression of metal ion-dependent enzyme genes, which possibly caused slightly increased CAT activity and decreased SOD activity in *OsNRAMP1*-OE plants, thereby resulting in compromised $H_2O_2$ (Figure 4). However, so far, it is unclear whether decreased $H_2O_2$ alters ROS homoeostasis, resulting in increased susceptibility to pathogens, at least in plants (Smirnoff & Arnaud, 2019). This is a possible reason explaining that *OsNRAMP1*-OE plants show no phenotypes after bacterial and fungal pathogen infection. In addition, the expressions of *OsNRAMP3* and *OsNRAMP7* were decreased in *OsNRAMP1*-OE plants (Figure S3). *OsNRAMP3* expression is induced by pathogens and it has a similar

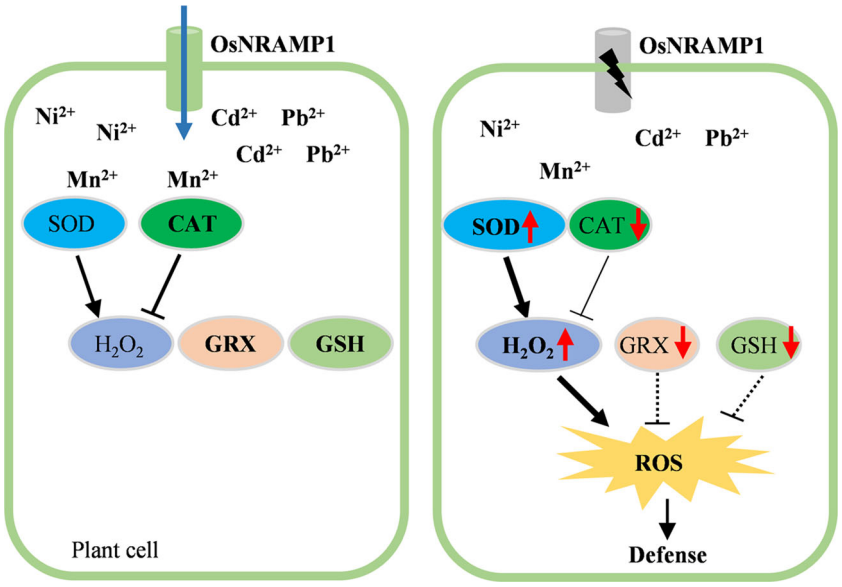


**FIGURE 10** A model of OsNRAMP1 functions in heavy-metal ion transportation and plant immunity. OsNRAMP1 acts as a multiple metal ion transporter transporting Mn, Ni, Cd and Pb in rice. Knockout of *OsNRAMP1* decreases the contents of these metal ions and reprogrammes metal ion-dependent enzyme activity, causing reactive oxygen species (ROS) burst, thereby triggering broad-spectrum disease resistance. The blue arrow indicates metal ion transportation. Black arrows indicate positive regulation, and blunt-ended bars indicate inhibition. Red arrows indicate increased or decreased levels [Color figure can be viewed at wileyonlinelibrary.com]

expression pattern as *OsNRAMP1* or *OsNRAMP6* upon pathogen infection (Zhou & Yang, 2004). Therefore, whether *OsNRAMP3* or *OsNRAMP7* complement *OsNRAMP1*-overexpressing conferred potential susceptibility is unknown. Furthermore, we could not exclude the possibility that accumulated metal ions, altered metal ion-dependent enzyme activity, reprogrammed gene expression of metal transporters and modulated ROS homoeostasis may potentially prolong the developing stage, promote chlorophyll content accumulation and even indirectly influence defence response of *OsNRAMP1*-OE plants.

### 4.3 | Engineering broad-spectrum disease resistance and toxic metal-safe rice via knockout of *OsNRAMP1*

Rice plants uptake mineral elements from soil by root, and then transport them to the shoot for rice growth and development, or to grains for normal development. The stored toxic elements in grains can be a direct threat to the health of humans. Therefore, it is extremely important to reduce toxic elements in edible parts of rice for human health. OsNRAMP1, acting as a multiple metal ion transporter, can transport Cd, Mn, Pb and Ni. Knockout of *OsNRAMP1* could significantly reduce the contents of Cd, Mn, Pb and Ni in grains. Moreover, the *osnramp1* mutant showed only a slight side-effect on major agronomic traits (Figure 9).

In conclusion, the results from the present study together with previously published data show that OsNRAMP1 is a multiple metal ion transporter. Knockout of *OsNRAMP1* not only regulates resistance of rice against various pathogens but also reduces the accumulation of toxic heavy elements in grains. Thus, the strategy of deletion of *OsNRAMP1* could provide a potential approach for engineering broad-spectrum disease resistance and toxic metal-safe rice.

## ACKNOWLEDGMENTS

We thank Prof. Xingming Lian and Dr. Meng Yang from Huazhong Agricultural University for technical assistance. This study was supported by grants from the National Natural Science Foundation of China (31821005, 31871946, 32172421), the National Science Foundation of Hubei Province (2020CFA058) and the Fundamental Research Funds for the Central Universities (2662019FW006).

## CONFLICT OF INTERESTS

The authors declare that there are no conflict of interests.

## DATA AVAILABILITY STATEMENT

The RNA-seq data from this study are deposited in the NCBI Sequence Read Archive (BioProject ID: PRJNA726296).

## ORCID

*Meng Yuan* http://orcid.org/0000-0003-1381-9202

## REFERENCES

Alejandro, S., Höller, S., Meier, B. & Peiter, E. (2020) Manganese in plants: from acquisition to subcellular allocation. *Frontiers in Plant Science*, 11, 300.

Arnon, D. (1949) Copper enzymes in isolated chloroplasts. polyphenoloxidase in *Beta vulgaris*. *Plant Physiology*, 24, 1–15.

Blackwell, J.M., Goswami, T., Evans, C.A., Sibthorpe, D., Papo, N., White, J.K. et al. (2001) SLC11A1 (formerly NRAMP1) and disease resistance. *Cellular Microbiology*, 3, 773–784.

Bozzi, A.T. & Gaudet, R. (2021) Molecular mechanism of Nramp-family transition metal transport. *Journal of Molecular Biology*, 433, 166991.

Broadley, M., Brown, P., Cakmak, I., Rengel, Z. & Zhao, F. (2012) *Function of nutrients: micronutrients, in marschner's mineral nutrient of higher plants*, 3rd edition. Oxford, pp. 191–249.

Cailliatte, R., Lapeyre, B., Briat, J.F., Mari, S. & Curie, C. (2009) The NRAMP6 metal transporter contributes to cadmium toxicity. *Biochemical Journal*, 422, 217–228.

Chang, J.D., Huang, S., Yamaji, N., Zhang, W., Ma, J.F. & Zhao, F.J. (2020) OsNRAMP1 transporter contributes to cadmium and manganese uptake in rice. *Plant Cell Environment*, 43, 2476–2491.

Clemens, S. & Ma, J.F. (2016) Toxic heavy metal and metalloid accumulation in crop plants and foods. *Annual Review of Plant Biology*, 67, 489–512.

Curie, C., Alonso, J.M., Le Jean, M., Ecker, J.R. & Briat, J.F. (2000) Involvement of NRAMP1 from *Arabidopsis thaliana* in iron transport. *Biochemical Journal*, 347, 749–755.

Descalsota, G., Swamy, B., Zaw, H., Inabangan-Asilo, M.A., Amparado, A., Mauleon, R. et al. (2018) Genome-wide association mapping in a rice MAGIC plus population detects QTLs and genes useful for biofortification. *Frontiers in Plant Science*, 9, 1347.

Fones, H. & Preston, G.M. (2013) The impact of transition metals on bacterial plant disease. *FEMS Microbiology Reviews*, 37, 495–519.

Garg, R., Jhanwar, S., Tyagi, A.K. & Jain, M. (2010) Genome-wide survey and expression analysis suggest diverse roles of glutaredoxin gene family members during development and response to various stimuli in rice. *DNA Research*, 17, 353–367.

Gunshin, H., Mackenzie, B., Berger, U.V., Gunshin, Y., Romero, M.F., Boron, W.F. et al. (1997) Cloning and characterization of a mammalian proton-coupled metal-ion transporter. *Nature*, 388, 482–488.

Hong, H., Liu, Y., Zhang, H., Xiao, J., Li, X. & Wang, S. (2015) Small RNAs and gene network in a durable disease resistance gene-mediated defense responses in rice. *PLOS One*, 10, e0137360.

Huang, S., Wang, P., Yamaji, N. & Ma, J.F. (2020) Plant nutrition for human nutrition: hints from rice research and future perspectives. *Molecular Plant*, 13, 825–835.

Hui, S., Shi, Y., Tian, J., Wang, L., Li, Y., Wang, S. et al. (2019) TALE-carrying bacterial pathogens trap host nuclear import receptors for facilitation of infection of rice. *Molecular Plant Pathology*, 20, 519–532.

Ishimaru, Y., Masuda, H., Bashir, K., Inoue, H., Tsukamoto, T., Takahashi, M. et al. (2010) Rice metal-nicotianamine transporter, OsYSL2, is required for the long-distance transport of iron and manganese. *The Plant Journal*, 62, 379–390.

Kaur, G. & Pati, P.K. (2016) Analysis of cis-acting regulatory elements of respiratory burst oxidase homolog (*Rboh*) gene families in *Arabidopsis* and rice provides clues for their diverse functions. *Computational Biology and Chemistry*, 62, 104–118.

Lanquar, V., Lelièvre, F., Bolte, S., Hamès, C., Alcon, C., Neumann, D. et al. (2005) Mobilization of vacuolar iron by AtNRAMP3 and AtNRAMP4 is essential for seed germination on low iron. *The EMBO Journal*, 24, 4041–4051.

Lee, S., Kim, Y.Y., Lee, Y. & An, G. (2007) Rice P1B-type heavy-metal ATPase, OsHMA9, is a metal efflux protein. *Plant Physiology*, 145, 831–842.

Li, J., Wang, Y., Zheng, L., Li, Y., Zhou, X., Li, J. et al. (2019) The intracellular transporter AtNRAMP6 is involved in Fe homeostasis in *Arabidopsis*. *Frontiers in Plant Science*, 10, 1124.

Li, J.Y., Liu, J., Dong, D., Jia, X., McCouch, S.R. & Kochian, L.V. (2014) Natural variation underlies alterations in Nramp aluminum transporter (*NRAT1*) expression and function that play a key role in rice aluminum tolerance. *Proceedings of the National Academy of Sciences of the United States of America*, 111, 6503–6508.

Li, Y., Cao, X.L., Zhu, Y., Yang, X.M., Zhang, K.N., Xiao, Z.Y. et al. (2019) Osa-miR398b boosts $H_2O_2$ production and rice blast disease-resistance via multiple superoxide dismutases. *New Phytologist*, 222, 1507–1522.

Li, Y., Li, J., Yu, Y., Dai, X., Gong, C., Gu, D. et al. (2021) The tonoplast-localized transporter OsNRAMP2 is involved in Fe homeostasis and affects seed germination in rice. *Journal of Experimental Botany*, 72, 4839–4852.

Liu, Y., Cao, Y., Zhang, Q., Li, X. & Wang, S. (2018) A cytosolic triosephosphate isomerase is a key component in XA3/XA26-mediated resistance. *Plant Physiology*, 178, 923–935.

Lv, Y., Shao, G., Jiao, G., Sheng, Z., Xie, L., Hu, S. et al. (2021) Targeted mutagenesis of *POLYAMINE OXIDASE 5* that negatively regulates mesocotyl elongation enables the generation of direct-seeding rice with improved grain yield. *Molecular Plant*, 14, 344–351.

Ma, G., Li, J., Li, J., Li, Y., Gu, D., Chen, C. et al. (2018) OsMTP11, a trans-Golgi network localized transporter, is involved in manganese tolerance in rice. *Plant Science*, 274, 59–69.

Ma, X., Zhang, Q., Zhu, Q., Liu, W., Chen, Y., Qiu, R. et al. (2015) A robust CRISPR/Cas9 system for convenient, high-efficiency multiplex genome editing in monocot and dicot plants. *Molecular Plant*, 8, 1274–1284.

Mani, A. & Sankaranarayanan, K. (2018) In silico analysis of natural resistance-associated macrophage protein (NRAMP) family of transporters in rice. *The protein journal*, 37, 237–247.

Miller, G., Suzuki, N., Ciftci-Yilmaz, S. & Mittler, R. (2010) Reactive oxygen species homeostasis and signalling during drought and salinity stresses. *Plant Cell Environment*, 33, 453–467.

Nagano, M., Ishikawa, T., Fujiwara, M., Fukao, Y., Kawano, Y., Kawai-Yamada, M. et al. (2016) Plasma membrane microdomains are essential for Rac1-RbohB/H-mediated immunity in rice. *The Plant Cell*, 28, 1966–1983.

Park, C.H., Chen, S., Shirsekar, G., Zhou, B., Khang, C.H., Songkumarn, P. et al. (2012) The *Magnaporthe oryzae* effector AvrPiz-t targets the RING E3 ubiquitin ligase APIP6 to suppress pathogen-associated molecular pattern-triggered immunity in rice. *The Plant Cell*, 24, 4748–4762.

Peris-Peris, C., Serra-Cardona, A., Sánchez-Sanuy, F., Campo, S., Ariño, J. & San Segundo, B. (2017) Two NRAMP6 isoforms function as iron and manganese transporters and contribute to disease resistance in rice. *Molecular Plant-Microbe Interactions*, 30, 385–398.

Rose, P.P., Hanna, S.L., Spiridigliozzi, A., Wannissorn, N., Beiting, D.P., Ross, S.R. et al. (2011) Natural resistance-associated macrophage protein is a cellular receptor for Sindbis virus in both insect and mammalian hosts. *Cell Host & Microbe*, 10, 97–104.

Rouhier, N., Lemaire, S.D. & Jacquot, J.P. (2008) The role of glutathione in photosynthetic organisms: emerging functions for glutaredoxins and glutathionylation. *Annual review of plant biology*, 59, 143–166.

Sasaki, A., Yamaji, N., Yokosho, K. & Ma, J.F. (2012) Nramp5 is a major transporter responsible for manganese and cadmium uptake in rice. *The Plant Cell*, 24, 2155–2167.

Segond, D., Dellagi, A., Lanquar, V., Rigault, M., Patrit, O., Thomine, S. et al. (2009) *NRAMP* genes function in *Arabidopsis thaliana* resistance to *Erwinia chrysanthemi* infection. *The Plant Journal*, 58, 195–207.

Shi, S., Wang, T., Chen, Z., Tang, Z., Wu, Z., Salt, D.E. et al. (2016) OsHAC1;1 and OsHAC1;2 function as arsenate reductases and regulate arsenic accumulation. *Plant Physiology*, 172, 1708–1719.

Shi, X., Long, Y., He, F., Zhang, C., Wang, R., Zhang, T. et al. (2018) The fungal pathogen *Magnaporthe oryzae* suppresses innate immunity by modulating a host potassium channel. *PLOS Pathogens*, 14, e1006878.

Smirnoff, N. & Arnaud, D. (2019) Hydrogen peroxide metabolism and functions in plants. *New Phytologist*, 221, 1197–1214.

Song, J.H., Wei, W., Lv, B., Lin, Y., Yin, W.X., Peng, Y.L. et al. (2016) Rice false smut fungus hijacks the rice nutrients supply by blocking and mimicking the fertilization of rice ovary. *Environmental Microbiology*, 18, 3840–3849.

Sun, X., Cao, Y., Yang, Z., Xu, C., Li, X., Wang, S. et al. (2004) *Xa26*, a gene conferring resistance to *Xanthomonas oryzae* pv. *oryzae* in rice, encodes an LRR receptor kinase-like protein. *The Plant Journal*, 37, 517–527.

Takahashi, R., Ishimaru, Y., Senoura, T., Shimo, H., Ishikawa, S., Arao, T. et al. (2011) The OsNRAMP1 iron transporter is involved in Cd accumulation in rice. *Journal of Experimental Botany*, 62, 4843–4850.

Thomine, S., Lelièvre, F., Debarbieux, E., Schroeder, J.I. & Barbier-Brygoo, H. (2003) AtNRAMP3, a multispecific vacuolar metal transporter involved in plant responses to iron deficiency. *The Plant Journal*, 34, 685–695.

Tiwari, M., Sharma, D., Dwivedi, S., Singh, M., Tripathi, R.D. & Trivedi, P.K. (2014) Expression in *Arabidopsis* and cellular localization reveal

involvement of rice NRAMP, *OsNRAMP1*, in arsenic transport and tolerance. *Plant Cell. Environment*, 37, 140–152.

Uraguchi, S., Kamiya, T., Sakamoto, T., Kasai, K., Sato, Y., Nagamura, Y. et al. (2011) Low-affinity cation transporter (OsLCT1) regulates cadmium transport into rice grains. *Proceedings of the National Academy of Sciences of the United States of America*, 108, 20959–20964.

Wang, J., Liu, X., Zhang, A., Ren, Y., Wu, F., Wang, G. et al. (2019) A cyclic nucleotide-gated channel mediates cytoplasmic calcium elevation and disease resistance in rice. *Cell Research*, 29, 820–831.

Wang, L., Xie, W., Chen, Y., Tang, W., Yang, J., Ye, R. et al. (2010) A dynamic gene expression atlas covering the entire life cycle of rice. *The Plant Journal*, 61, 752–766.

Xu, G., Yuan, M., Ai, C., Liu, L., Zhuang, E., Karapetyan, S. et al. (2017) uORF-mediated translation allows engineered plant disease resistance without fitness costs. *Nature*, 545, 491–494.

Yamaji, N., Sasaki, A., Xia, J.X., Yokosho, K. & Ma, J.F. (2013) A node-based switch for preferential distribution of manganese in rice. *Nature Communications*, 4, 2442.

Yan, H., Xu, W., Xie, J., Gao, Y., Wu, L., Sun, L. et al. (2019) Variation of a major facilitator superfamily gene contributes to differential cadmium accumulation between rice subspecies. *Nature Communications*, 10, 2562.

Yang, M., Lu, K., Zhao, F.J., Xie, W., Ramakrishna, P., Wang, G. et al. (2018) Genome-wide association studies reveal the genetic basis of ionomic variation in rice. *The Plant Cell*, 30, 2720–2740.

Yang, W., Guo, Z., Huang, C., Duan, L., Chen, G., Jiang, N. et al. (2014) Combining high-throughput phenotyping and genome-wide association studies to reveal natural genetic variation in rice. *Nature Communications*, 5, 5087.

Yocum, C.F. & Pecoraro, V.L. (1999) Recent advances in the understanding of the biological chemistry of manganese. *Current Opinion in Chemical Biology*, 3, 182–187.

Yuan, M., Chu, Z., Li, X., Xu, C. & Wang, S. (2010) The bacterial pathogen *Xanthomonas oryzae* overcomes rice defenses by regulating host copper redistribution. *The Plant Cell*, 22, 3164–3176.

Yuan, M., Ke, Y., Huang, R., Ma, L., Yang, Z., Chu, Z. et al. (2016) A host basal transcription factor is a key component for infection of rice by TALE-carrying bacteria. *eLife*, 5, e19605.

Zhang, Y., Xu, Y.H., Yi, H.Y. & Gong, J.M. (2012) Vacuolar membrane transporters OsVIT1 and OsVIT2 modulate iron translocation between flag leaves and seeds in rice. *The Plant Journal*, 72, 400–410.

Zhou, X. & Yang, Y. (2004) Differential expression of rice *Nramp* genes in response to pathogen infection, defense signal molecules and metal ions. *Physiological and Molecular Plant Pathology*, 65, 235–243.

## SUPPORTING INFORMATION

Additional supporting information may be found in the online version of the article at the publisher's website.

**How to cite this article:** Chu, C., Huang, R., Liu, L., Tang, G., Xiao, J., Yoo, H. et al. (2022) The rice heavy-metal transporter OsNRAMP1 regulates disease resistance by modulating ROS homoeostasis. *Plant, Cell & Environment*, 45, 1109–1126. https://doi.org/10.1111/pce.14263

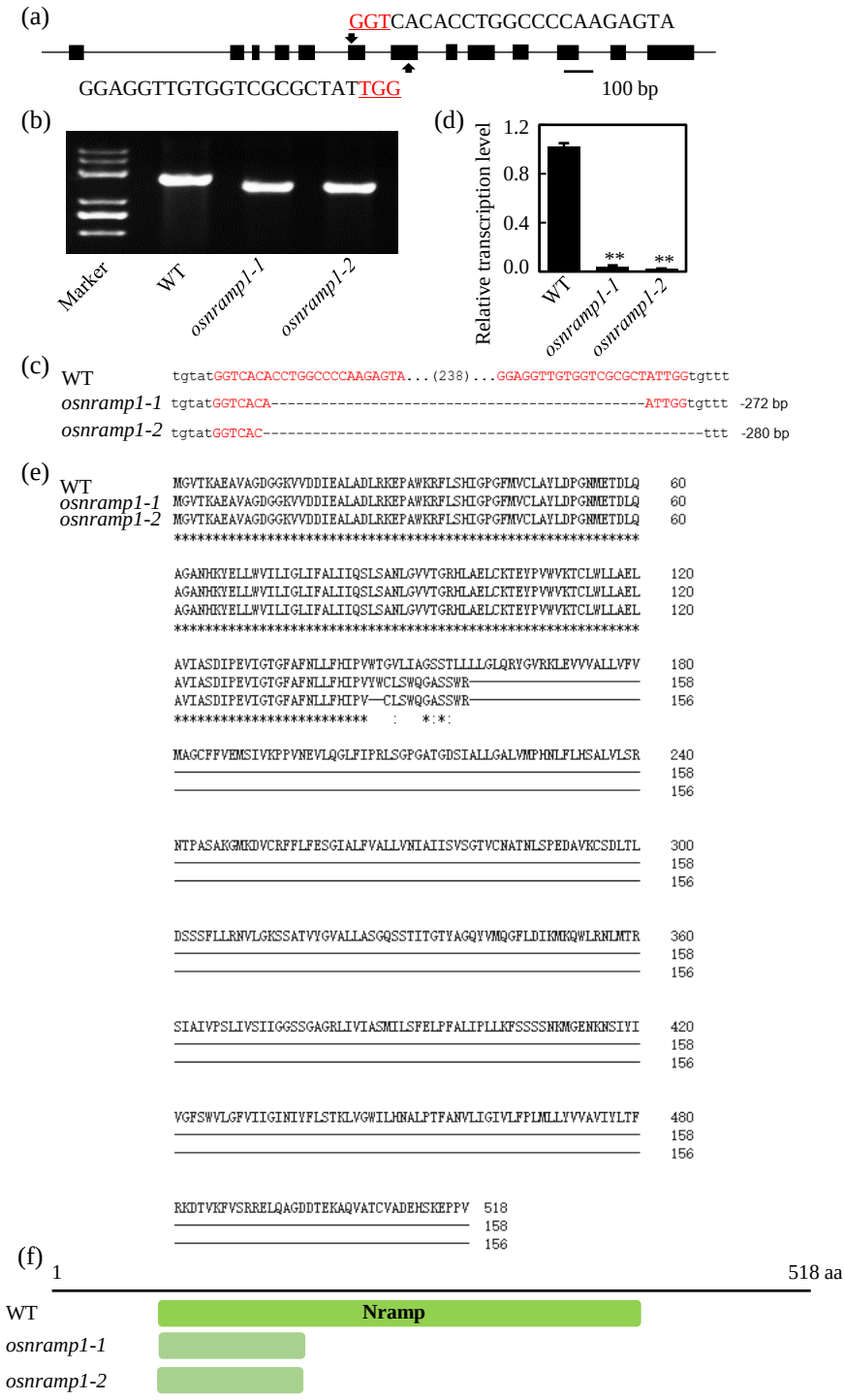


**FIGURE S1** Generation of *OsNRAMP1* knockout lines. (a) The target site designed for knocking out *OsNRAMP1* by the CRISPR/Cas9 strategy. The target site nucleotides are shown in capital letters, and the PAM site is indicated as red capital letters. (b) Gel electrophoresis of PCR products amplified from the mutant region. (c) Sequence alignment of the target regions showing large fragment deletion in two independent *osnramp1* plants. (d) Transcription level of *OsNRAMP1* in wild type (WT) and mutants. Data are means ± SD. Asterisks indicate significant differences between *osnramp1* mutants and WT determined by two-tailed Student's *t*-test (**$P$<0.01). (e) Amino acid alignment of OsNRAMP1 in WT and mutants. (f) The conserved Nramp domain (pfam01566) of OsNRAMP1 protein was destroyed in *osnramp1* plants.

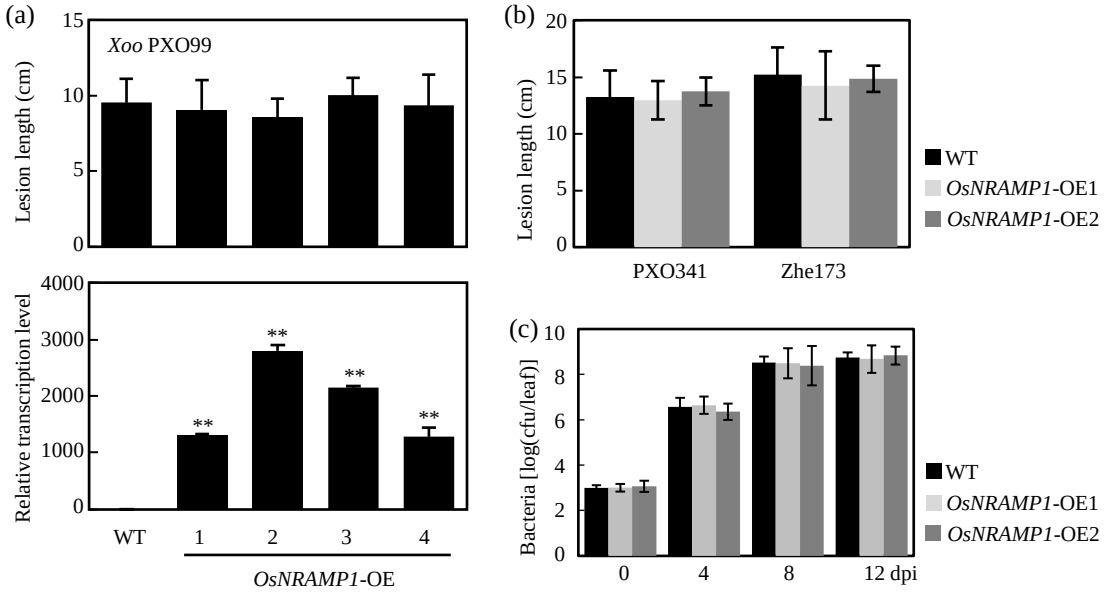


**FIGURE S2** Relative transcription levels of *OsNRAMP1* (a), lesion length (b), and *Xoo* growth (c) in *OsNRAMP1*-OE plants. Plants were inoculated with *Xoo* at booting stage. dpi, days post infection. Bar are mean ± SD. Asterisks indicate significant differences between *OsNRAMP1*-OE plants and wild type (WT) determined by two-tailed Student's *t*-test (***P*<0.01).

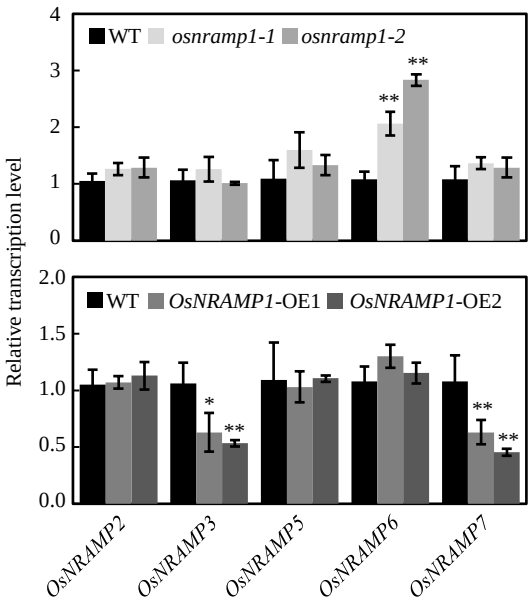


**FIGURE S3** Relative transcription level of *OsNRAMP* genes in leaves of *osnramp1* mutants and *OsNRAMP1*-OE plants. Bar are mean ± SD. Asterisks indicate significant differences between wild type (WT) and *osnramp1* mutants or *OsNRAMP1*-OE plants determined by two-tailed Student's *t*-test (***P*<0.01 or **P*<0.05).

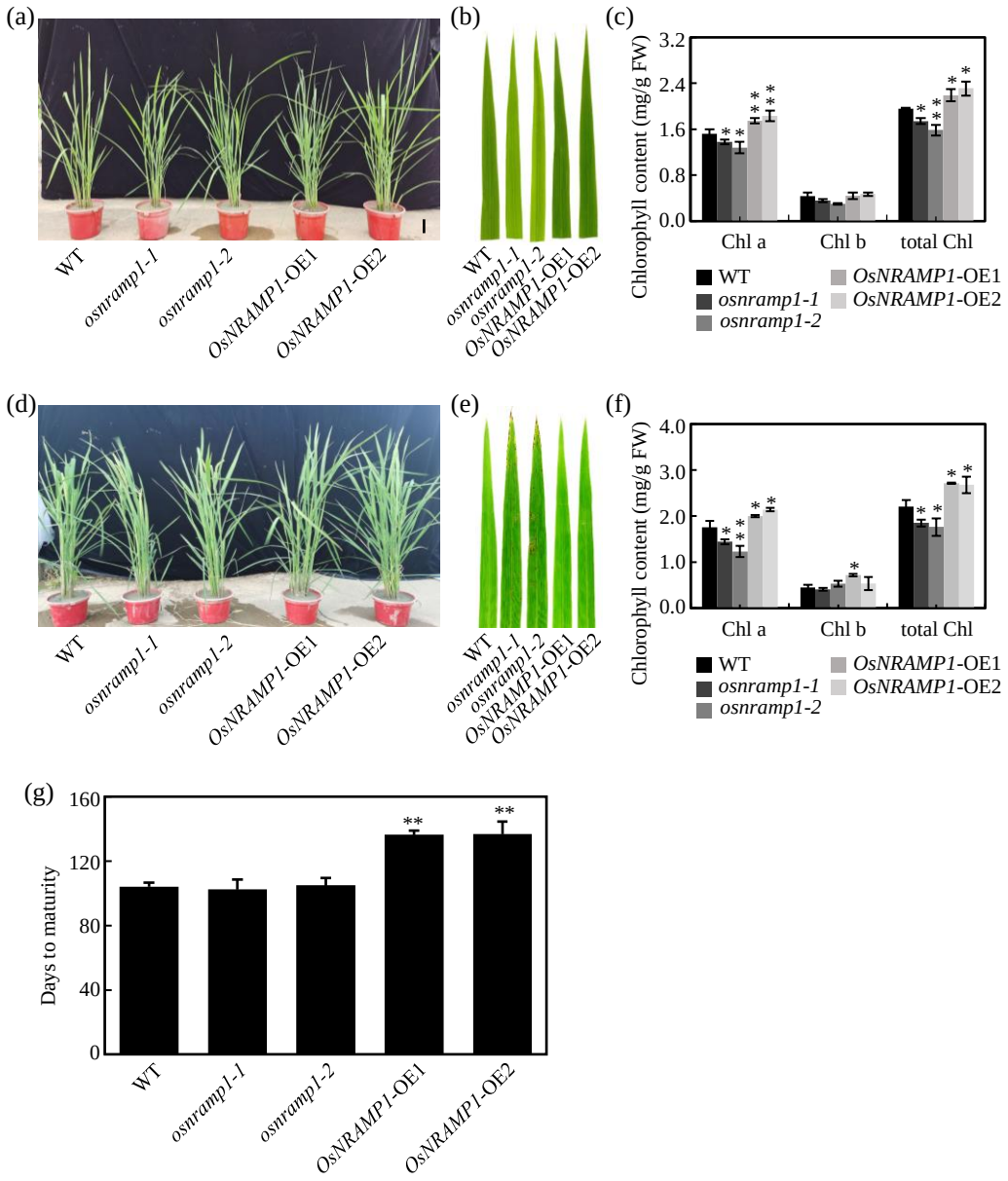


**FIGURE S4** Phenotypic analysis of *osnramp1* mutants, *OsNRAMP1*-OE plants and wild type (WT) grown in the paddy field. (a) The whole plant at tillering stage. (b) Leaf at tillering stage. (c) Leaf chlorophyll content at tillering stage. (d) The whole plant at booting stage. (e) Leaf at booting stage. (f) Leaf chlorophyll content at booting stage. (g) Comparison of maturity date under long-day condition. Bar are mean ± SD. Asterisks indicate significant difference determined by two-tailed Student's *t*-test (***P*<0.01 or **P*<0.05).

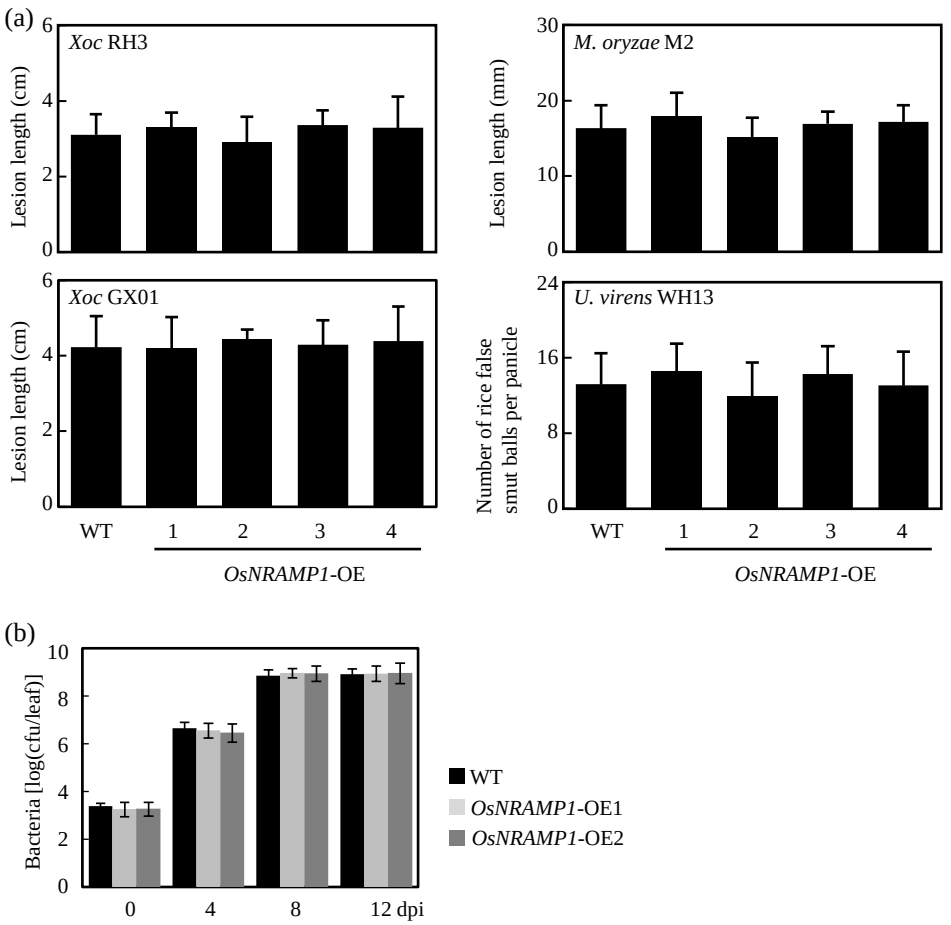


**FIGURE S5** Response of *OsNRAMP1*-OE plants to bacterial pathogen *Xoc*, fungal pathogens *M. oryzae* and *U. virens* (a) and *Xoc* growth (b). Plants were inoculated with *Xoo* RH3 and GX01 and *M. oryzae* M2 at tillering stage, *U. virens* WH13 at booting stage. dpi, days post infection. Bar are mean ± SD.

(a)

| | Gene number |
|---|---|
| Up-DEGs | 2542 |
| Down-DEGs | 3727 |
| Total | 6269 |

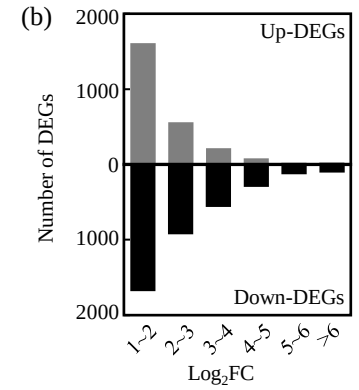


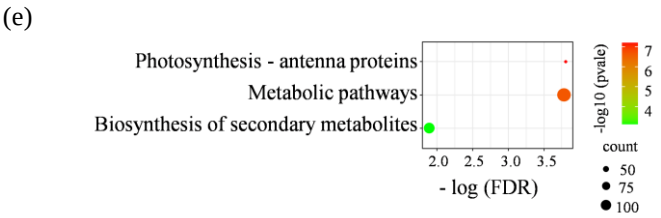


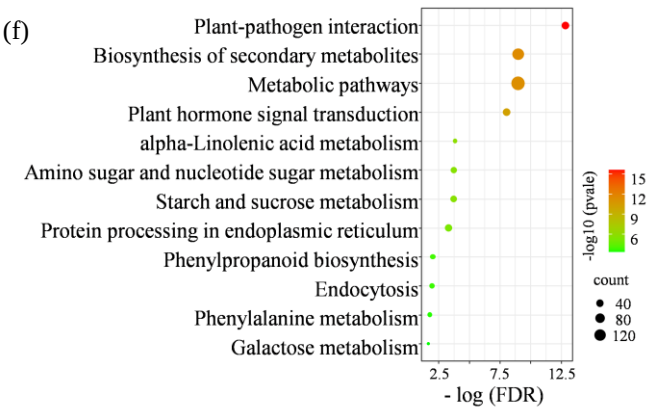


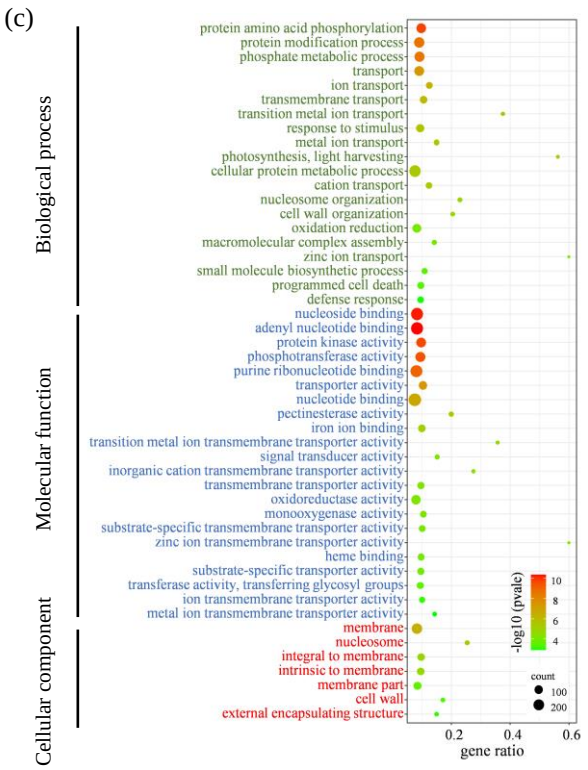


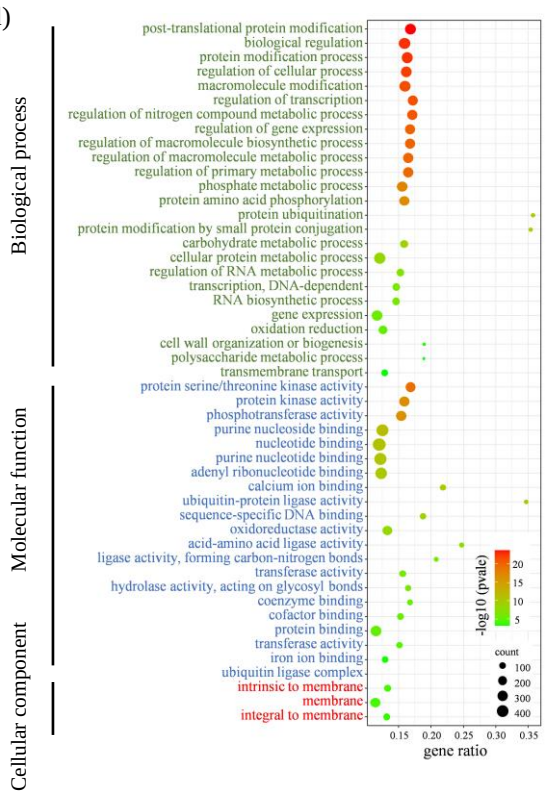


**FIGURE S6** GO enrichment and KEGG pathway analysis of *osnramp1* mutant DEGs. (a) The number of up-regulated and down-regulated DEGs. (b) Distribution of up-regulated and down-regulated DEGs with different fold changes. (c) GO enrichment analysis of up-regulated DEGs. (d) GO enrichment analysis of down-regulated DEGs. (e) KEGG enrichment analysis of up-regulated DEGs. (f) KEGG enrichment analysis of down-regulated DEGs. DEGs, differentially expressed genes.

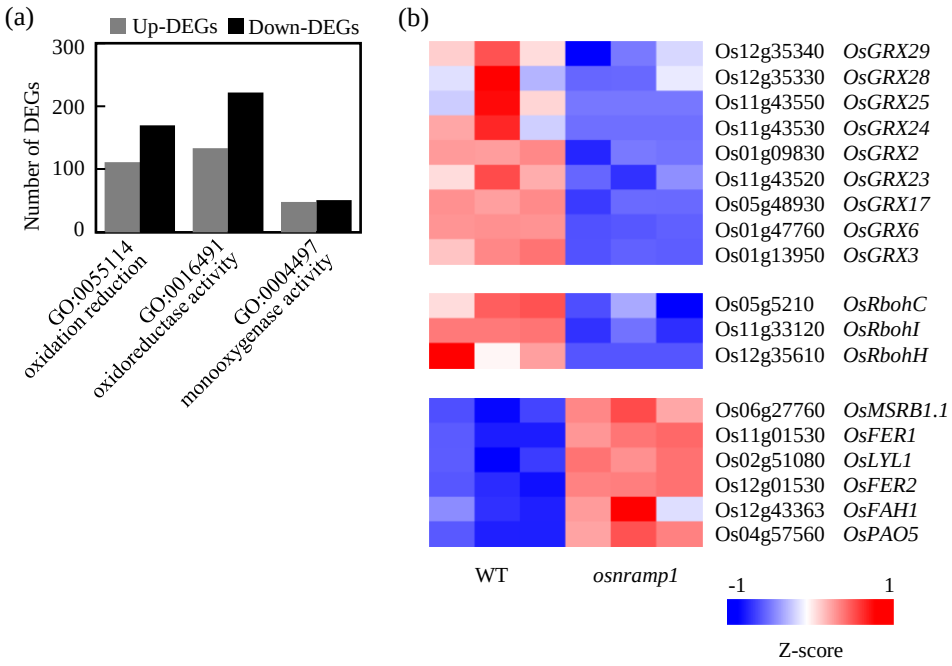


**FIGURE S7** Differentially expressed genes involving in reactive oxygen species. (a) The number of Up-DEGs and Down-DEGs that play roles in reactive oxygen species homeostasis. (b) The heat map of Up-DEGs and Down-DEGs involving in reactive oxygen species. DEGs, differentially expressed genes. WT, wild type.

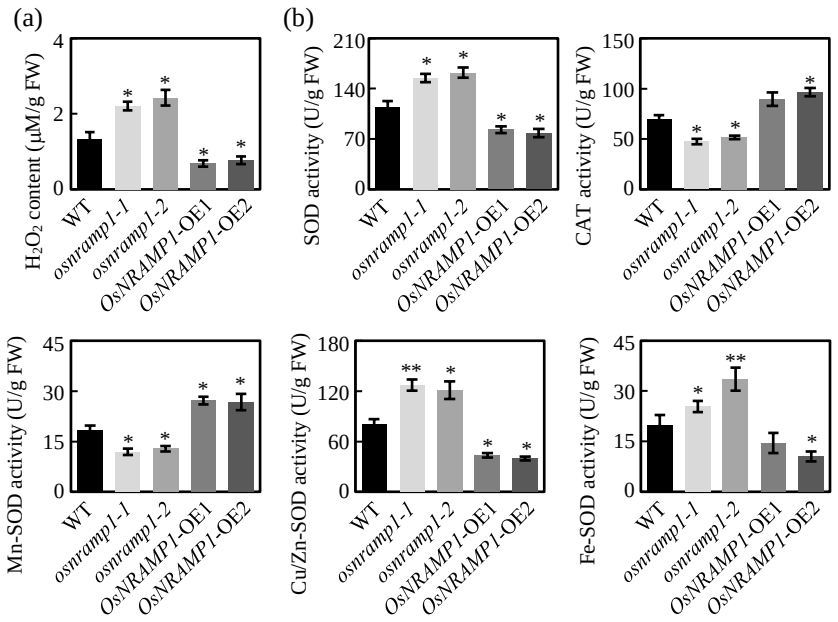


**FIGURE S8** Impaired reactive oxygen species homeostasis in panicle of *osnramp1* mutants. (a) $H_2O_2$ content in panicle of *osnramp1* mutants, *OsNRAMP1*-OE plants and wild type (WT). (b) The SOD, CAT, Mn-SOD, Cu/Zn-SOD and Fe-SOD activities in panicle of *osnramp1* mutants, *OsNRAMP1*-OE plants and wild type. Bar are mean ± SEM. Asterisks indicate significant differences between wild type and *osnramp1* mutants or *OsNRAMP1*-OE plants determined by two-tailed Student's *t*-test (***P*<0.01 or **P*<0.05).

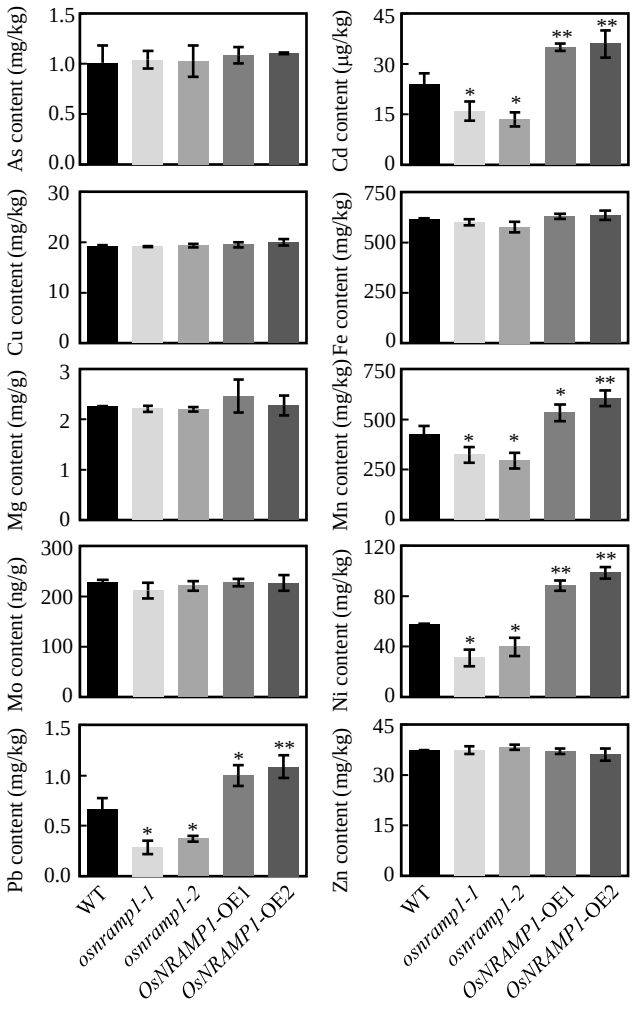


**FIGURE S9** Concentrations of As, Cd, Cu, Fe, Mg, Mn, Mo, Ni, Pb, and Zn in leaves of *osnramp1* mutants, *OsNRAMP1*-OE plants and wild type (WT) grown in the paddy field. Data are means (total 80 leaves from eight plants) ± SD. Asterisks indicate significant differences between wild type and *osnramp1* mutants or *OsNRAMP1*-OE plants determined by two-tailed Student's *t*-test (***P*<0.01 or **P*<0.05).

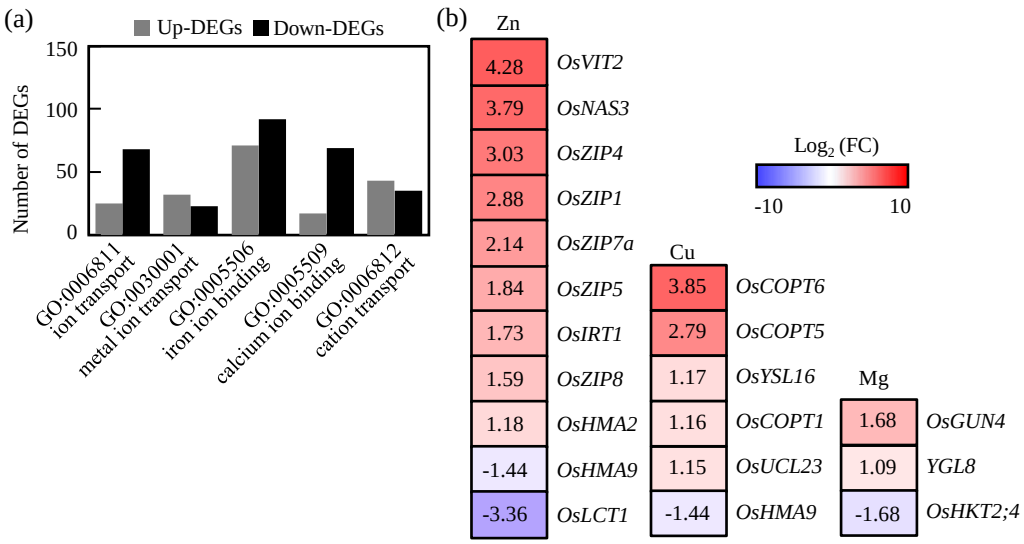


**FIGURE S10** Differentially expressed genes involving in metal uptake or transport. (a) The number of Up-DEGs and Down-DEGs that play roles in metal uptake or transport. (b) The heat map of Up-DEGs and Down-DEGs involving in uptake or transport for Zn, Cu and Mg. The number indicates the value ($Log_2$) of gene expression for *osnramp1* mutant compared with that for wild type. DEGs, differentially expressed genes.

**Table S1.** PCR primers used for vectors construction

| Gene | Forward primer (5'-3') | Reverse primer (5'-3') | Use |
|---|---|---|---|
| *OsNRAMP1* | GGCATGAGAACCCCGGTCCACACGTTTTAGAGCTAG | GTGTGGACCGGGGTTCTCATGCCACGGATCATCTGC | CRISPR construct |
| | GCCGGAGGTTGTGGTCGCGCTATGTTTTAGAGCTAG | ATAGCGCGACCACAACCTCCGGCAGCCAAGCCAGCAC | CRISPR construct |
| | TATCGGCTAATCTTGGAG | GTACACTGTCGCACTTGA | Mutant detection |
| | TACGAACGATAGCCGGTACCGGCAGAGATCGGGGTTCGGC | TGATCTTTGTAATCGGATCCCACGGGTGGCTCTTTGCTGT | Overexpressing construct |

**Table S2.** PCR primers used for RT-qPCR assay

| Gene | Forward primer (5'-3') | Reverse primer (5'-3') |
|---|---|---|
| *OsNRAMP1* | CTGCAAAGATATGGGGTAAGGA | GGTTAATGAGGTCCTTCAAGGA |
| *OsNRAMP2* | TTGGTGGTTCCAAAGTTGAGTTC | CATGATTATGCAGCCCACAATT |
| *OsNRAMP3* | GAGCGGCCCAATGCAA | CCGCTCGACGCTAGAGATAAA |
| *OsNRAMP5* | TGGGTCGGCGTCCTCAT | TTGGAGGCCAAGAAGCAGTAG |
| *OsNRAMP6* | GGTCTGCACGGCGATGTC | CAGGACCAACATGTGCAAGAA |
| *OsNRAMP7* | AGCGCTTGTTCAGTCGAGAAA | CAACGCTTCACGGACTTGGT |
| *OsHAC1;2* | TAGCATCTGCCGATCTCATA | GAGGTTTATTCACCGCAAGG |
| *OsHMA9* | TTGGCAAGCTCCCTACATCAA | GCCAGGCAAGGCAGAGAA |
| *OsMTP11* | CAGAAGTGAGGCATTAGC | AAGTGGAGGCAATTATAGC |

| | | |
|---|---|---|
| *OsYSL2* | GAGGGACAACGGTGTCATTGCTGGT | TGCAGAAAAGCCCTCGACGCCAAGA |
| *OsLCT1* | GAGTTCTTCGTCAGAGCTAC | CAGTGCTGGATGACGAATTG |
| *OsCd1* | TCAGCTGCATCACCAAGCACT | TCTCTTGTTGTGCTCCGCGA |
| *OsCSD1* | ACCAATGGTTGCATGTCAAC | TGAATTTGGTCCAGTAAGTGG |
| *OsCSD2* | AAGAGGAGAGGGTGGGCAAC | AGTTGACATGCAGCCATTAGTGG |
| *OsCSD3* | TGGGCGACCTGGGAAACATAG | GAGTTCATGACCACCCCTTCCT |
| *OsCSD4* | TCCGTGTGACGGGACTTAC | GCCTCAGCTACACCTTCAGCAT |
| *OsCatA* | AGGAGGCAGAAGGCGACGATACA | TCTTCACATGCTTGGCTTCACGTT |
| *OsCatB* | GGCTGTCGGGAAAAGTGTGTCATTG | TTTCAGGTTGAGACGTGAAGCCAGC |
| *OsCatC* | TCAAGAGATGGATCGACGCACTCTC | GAAGCAGATTGCAACGCTGATCG |
| *OsGAPDH* | CAATCGTGAGAAGATGACCC | GTCCATCAGGAAGCTCGTAGC |
| *OsMSD* | GGTGATCCACCACATGCAAA | CCTCAAATGAACCAAAATCCTCAT |
| *OsFSD1* | TGGATGGGTTTGGCTTTGTT | TGGGCTTCTTGATTTCACATGA |
| *OsFSD2* | TGCCATCAGTCCACTTGCA | GTAAGCATGCTCCCACAAGTCTAG |
| *OsGRX3* | CATGTCCCTTTTGATCTTTTTTAACTG | TGATCGACGCAATTAAAGATAGAATT |
| *OsGRX6* | CGTGCCATCGTGGTTCAAT | GAAATCCGCCGCGATGTA |
| *OsPRX126* | GCGCAGATGCCCACAAGT | TGCCCATCTTCACCATGGAT |
| *OsFAD7* | CGTGCTGGGTCACGACTGT | TGTTCAACTTGGCGTTGCTT |
| *OsBsr-d1* | CATCGAGTATGCAACAAGCTAAGCT | CCCTTGGCGACAATCAATCT |
| *OsGR3* | GGCCATCCATGCCAGACA | CCAATGCTGCATCTGAATCAA |
| *OsRbohH* | TGACAGCAACCCGCTGAAG | GACGAAGAGGTGGTGGGAGTAC |
| *OsGRX17* | GCACATGCGCTTGCAAAC | CACGGTAGCGGCGACAAC |
| *OsGRX23* | TTCTCAAGCACACAGTGATCGA | CGAGACCTGGAACCCCTTCT |
| *OsGRX2* | TGTCCCATCGTCGTCTTCCT | TGGAAGGCATGGAGCTAAGC |

| | | |
|---|---|---|
| *OsGRX24* | GATGGCCATGCACCTCAAG | AATCACAGTAATCTCAAAGCCACAGT |
| *OsRboh* | GCGTGAGGCCAGTGAAGATAC | GCAGCGACAGCACATTTCC |
| *OsDSM2* | CGCCGCCCACCAGATAC | CAGCCCATATGGCACACCTT |
| *OsGPX1* | ACCTCCGTCCACGACTTCAC | AGGTGCTCAGGTTCACGTCTTT |
| *OsRbohC* | GGAAGAACTGCGCGAGATCT | GGAGGCGCGAGTCGAA |
| *OsFAH2* | CCCCCTACTGCAACAGCAA | GCGAAGAACGCTACCAGCTT |
| *OsMSRB1.1* | CTGTGACACCCCTCTTTTTGAGT | ACGGCCACCCAGTACCACTA |
| *OsFER1* | CGTGACAACGTTGCTCTCAAG | TCCTCATCGCTGGATTCTTTG |
| *OsFER2* | CACTCCCTTTTCGCCTACTTTG | ATTTGGCGAATCCCTTGAGA |
| *OsFAH1* | TGACGGCCTTCGACTTGTC | CAGAACGGAAAGCACAAGATAGC |
| *OsPAO5* | GGTGGCCATGGGCTTATG | TCTTGCGCGAGAGCTTTGAT |
| *Osactin* | TGTATGCCAGTGGTCGTACCA | CCAGCAAGGTCGAGACGAA |